Journal of Statistical Physics, Vol. 102, Nos. 3/4, 2001

Wavevector-Dependent Susceptibility in Quasiperiodic Ising Models

Helen Au-Yang,[1] Bai-Qi Jin,[1] and Jacques H. H. Perk[1]

Received June 15, 2000

Using the various functional relations for correlation functions in planar Ising models, new results are obtained for the correlation functions and the q-dependent susceptibility for Ising models on a quadratic lattice with quasiperiodic coupling constants. The effects are clearest if the interactions are both attractive and repulsive according to a quasiperiodic pattern. In particular, an exact scaling limit result for the two-point correlation function of the Z-invariant inhomogeneous Ising model is presented and the q-dependent susceptibility is calculated for some cases where the coupling constants vary according to Fibonacci rules. It is found that the ferromagnetic case differs drastically from the case with both ferro- and antiferromagnetic bonds. In the mixed case, the peaks of the q-dependent susceptibility are everywhere dense for temperature T both above or below the critical temperature T_c, but due to overlap only a finite number of peaks is visible. This number of visible peaks decreases as T moves away from T_c. In the ferromagnetic case, there is typically only one single peak at $\mathbf{q} = 0$, in spite of the aperiodicity present in the lattice. These results provide evidence that in real systems, even if the atoms arrange themselves aperiodically, there will be no dramatic difference in the diffraction pattern, unless the pair correlation function has clear aperiodic oscillations. The number of oscillations per correlation length determines the number of visible peaks.

KEY WORDS: Ising model; Z-invariance; quasiperiodicity; Fibonacci; correlation functions; wavevector dependent susceptibility; scaling limit.

1. FOREWORD AND DEDICATION

As this paper is an expanded version of a talk presented at a conference to honor Dr. Rodney Baxter's sixtieth birthday, it seems proper to us to go back many years and to recall how the present research was started and how much we owe Dr. Baxter.

[1] Department of Physics, Oklahoma State University, Stillwater, Oklahoma 74078-3072.

0022-4715/01/0200-0501$19.50/0

While Baxter was visiting Stony Brook in 1980 one question came up a few times about the book[1] he was writing, namely why so little is said about correlation functions in his book. He replied with a challenge: Since you know so much about the correlation functions of the Ising model,[2–11] how does my result on p. 343 of ref. 12 fit in? Somehow, with very little input, Baxter was able to write down a formula for the two-point correlation function of the most general inhomogeneous Ising model solvable by commuting transfer matrices, which he named the Z-invariant Ising model.[12, 13]

Baxter's result for the two-point function, with $2m$ rapidity variables α_j passing between the two spins, is

$$
\begin{aligned}
&g_{2m}(k; \alpha_1, \ldots, \alpha_{2m}) \\
&\quad = \frac{1}{m!\, \mathrm{H}_1(0)} \left[-\frac{k^{1/2} \Theta^3(0)}{2\pi} \right]^m \prod_{1 \leqslant j < l \leqslant 2m} \Theta(\mathrm{i}\alpha_j - \mathrm{i}\alpha_l) \\
&\qquad \times \int_{-\mathrm{K}}^{\mathrm{K}} \mathrm{d}s_1 \cdots \int_{-\mathrm{K}}^{\mathrm{K}} \mathrm{d}s_m \, \frac{\prod_{1 \leqslant j < l \leqslant m} [\mathrm{H}^2(s_j - s_l)\, \Theta^2(s_j - s_l)]}{\prod_{r=1}^{2m} \prod_{j=1}^{m} [\mathrm{H}(s_j - \mathrm{i}\alpha_r)\, \Theta(s_j - \mathrm{i}\alpha_r)]} \\
&\qquad \times \Psi_m \left(\sum_{l=1}^{m} (2s_l - \mathrm{i}\alpha_{2l-1} - \mathrm{i}\alpha_{2l}) \right)
\end{aligned}
\tag{1.1}
$$

where

$$
\Psi_m(u) = \begin{cases} \Theta_1(u), & \text{if} \quad m = \text{odd} \\ \mathrm{H}_1(u), & \text{if} \quad m = \text{even} \end{cases} \tag{1.2}
$$

k is the elliptic modulus, K the complete elliptic integral of the first kind, and Θ, H, Θ_1, and H_1 are Jacobi theta functions.

Years later Baxter repeated the challenge[14] to two of us and soon after we were able to derive his result, restricted to the critical temperature at first, starting from quadratic recurrence relations[15] for general planar Ising models expressing the fermionic nature[3, 4] of the model. As a byproduct we obtained several other determinant and Pfaffian representations[16, 17] for the correlation function of the Z-invariant Ising model. More recently, Reyes Martínez[18, 19] derived the above formula (1.1) and further Pfaffian results while starting from the vertex operator approach.[20, 21]

The agreement between these three different methods provides very strong support for the validity of this vertex operator approach and opens the door to applications. The original result (1.1), as Baxter has said it himself,[12] is "rather unwieldy," not easily analyzed. But the Z-invariant

Ising model is an attractive exactly solvable model for studying quasicrystals and quasiperiodic systems.[22–29]

Therefore, we dedicate the current work, flowing forth from our attempt to apply what we learned from Baxter to calculate the structure function of Z-invariant quasiperiodic systems, as a birthday present to Dr. Baxter.

2. INTRODUCTION

The wavevector-dependent susceptibility $\chi(\mathbf{q})$ is in many ways similar to the static structure factor $S(\mathbf{q}) = \langle \hat{\rho}(\mathbf{q})\, \hat{\rho}(-\mathbf{q}) \rangle$, with $\hat{\rho}(\mathbf{q})$ the Fourier transform of the local density $\rho(\mathbf{r})$. Just like $S(\mathbf{q})$, $\chi(\mathbf{q})$ gives information on the average relative locations of the atoms. It can also be determined experimentally and for the Ising model $\chi(\mathbf{q})$ even translates into the static structure factor of the equivalent lattice gas model.

Since $\chi(\mathbf{q})$ is a sum of spin correlation functions, at this time it cannot be explicitly calculated in most of the solvable models of statistical mechanics. One exception[2] to be considered in the current work is the two-dimensional Ising model whose correlation functions have been intensively studied by many authors.[4, 7–19, 31–38]

More specifically, we shall study exactly the q-dependent susceptibility of certain Fibonacci Ising models in order to obtain some insight in the theory of aperiodic crystals. Since these are very crude models, one does not expect them to represent any existing physical systems, even though with modern experimental techniques one should be able to grow crystals that are well approximated by them.

Here we choose to study only those models whose correlation functions can be related to the one of the regular Ising model. This then excludes the models considered by Tracy[39, 40] that are not Z-invariant. Our crude models can nevertheless be used to gain theoretical understanding as to what is the most important factor that would reproduce the infinitely many and everywhere dense peaks in the q-dependent susceptibility, or in the diffraction patterns[41–43] in quasicrystals. The following are the points we would like to consider.

2.1. Aperiodic as Limit of Periodic

When it was discovered that there is a clear five-fold symmetry in the diffraction patterns[44] of a certain alloy, which is a symmetry incompatible

[2] Another exception is, of course, one-dimensional models in which structure functions can be calculated by various methods such as exact renormalization group calculations.[30]

with any crystallographic space group, this alloy was called an icosahedral quasicrystal.[44, 45] In order to explain this, Pauling then suggested that this was caused by a crystal structure with a gigantic unit cell,[46] which can also have such a five-fold symmetry.

To gain some theoretical understanding of this problem, we study the wavevector-dependent susceptibility of a sequence of Ising lattices whose edge interactions take different—either positive or negative—values periodically and aperiodically. More specifically, the aperiodic lattice is a limiting case of a sequence of periodic lattices whose period F_n is the nth element in the Fibonacci sequence, satisfying the defining relation

$$F_{n+1} = F_n + F_{n-1}, \qquad F_0 = F_1 = 1 \tag{2.1}$$

We shall compare the results for the periodic case with period F_n with the aperiodic case with $F_n \to \infty$ for different correlation lengths. This may shed some light on the difference of assuming that the system is quasiperiodic or just a system with a large unit cell.

2.2. Order Versus Disorder

To understand why the randomized icosahedral system[47] gives almost the same diffraction pattern as a quasicrystal, we study the q-dependent susceptibility for $T > T_c$ and $T < T_c$. Since above T_c the system is in a disordered state, whereas below T_c the system is in an ordered state, this contrast may enable us to determine whether the distinction that the system is ordered or disordered is indeed irrelevant.

2.3. Mixed Attractive and Repulsive Interactions

Many of the earlier results on Ising models on Penrose tilings[26, 28, 48, 49] and on the Fibonacci Ising chain[50] all assumed ferromagnetic couplings only and it was found that they belong to the same universality class as the periodic case without finding real interesting results. We study here the q-dependent susceptibility for both ferromagnetic and mixed Fibonacci Ising lattices. The contrast of the susceptibilities of the two cases—one with ferromagnetic bonds only, the other with antiferromagnetic bonds also—is remarkable, however.

2.4. Outline

The paper is organized as follows. First, in Section 3 we present some definitions and a system of quadratic relations[15] for the pair correlation

function in the uniform and symmetric Ising model. In Section 4 we explain how we compute the diagonal correlation functions for the uniform case, either using Toeplitz determinants or the method of Jimbo and Miwa.[36] In Section 5 we present our results for the wavevector-dependent susceptibility in the Fibonacci Ising model with ferro- and antiferromagnetic interactions of equal strength with signs given by Fibonacci sequences. Next, in Section 6 we derive the scaled pair correlation function for Baxter's inhomogeneous Z-invariant Ising model. We use these results to give some discussion of the purely ferromagnetic Z-invariant Ising model with couplings of unequal strength in Section 7. Finally, we present our conclusions in Section 8.

3. DEFINITIONS AND QUADRATIC RECURRENCE RELATIONS

In this section we briefly review some old results in order to fix notations.

3.1. Symmetric Uniform Ising Model on Quadratic Lattice

The symmetric two-dimensional Ising model is defined by the interaction energy

$$\mathscr{E} = -J \sum_{m,n} (\sigma_{m,n}\sigma_{m,n+1} + \sigma_{m,n}\sigma_{m+1,n}) \tag{3.1}$$

For this model it is convenient to define the elliptic modulus[2]

$$k = \sinh^2(2J/k_{\mathrm{B}}T) \tag{3.2}$$

which satisfies $k<1$ for $T>T_{\mathrm{c}}$ and $k>1$ for $T<T_{\mathrm{c}}$, with $k \to 1/k$ giving the Kramers–Wannier duality transformation.

The spontaneous magnetization is simply given by[5–7, 10]

$$\langle \sigma \rangle = \begin{cases} (1-k^{-2})^{1/8}, & T<T_{\mathrm{c}} \\ 0, & T \geqslant T_{\mathrm{c}} \end{cases} \tag{3.3}$$

The calculation of the pair correlation function $C(m,n)$ and the connected pair correlation function $C^{(\mathrm{c})}(m,n)$, defined by

$$C(m,n) = \langle \sigma_{0,0}\sigma_{m,n} \rangle \qquad \text{and} \qquad C^{(\mathrm{c})}(m,n) = \langle \sigma_{0,0}\sigma_{m,n} \rangle - \langle \sigma \rangle^2 \tag{3.4}$$

is non-trivial. Already a long time ago, this correlation function $C(m,n)$ has been expressed in terms of determinants[4, 7, 10] of size proportional to the distance of the spins.

But such an expression is not that useful for calculating wavevector-dependent susceptibilities

$$\chi(q_x, q_y) = \frac{1}{\mathcal{N} k_{\mathrm{B}} T} \sum_{m_1, n_1} \sum_{m_2, n_2} \mathrm{e}^{\mathrm{i}q_x(m_1 - m_2) + \mathrm{i}q_y(n_1 - n_2)} \times (\langle \sigma_{m_1, n_1} \sigma_{m_2, n_2} \rangle - \langle \sigma_{m_1, n_1} \rangle \langle \sigma_{m_2, n_2} \rangle) \tag{3.5}$$

unless the correlation length is extremely small. Here $\mathcal{N}$ is the number of sites of the lattice and we have given the expression in a form that it is valid for nonuniform lattices also.

We will show in a later section that we can obtain interesting quasicrystal behavior by using a gauge transformation making the interactions ferro- or antiferromagnetic according to Fibonacci sequences. But, in order to see many peaks, the correlation length can not be small. Even though many papers on Fibonacci Ising models have been written, to our knowledge, no susceptibility calculations have been reported.

3.2. Quadratic Identities for Two-Point Correlation Function

We can avoid calculating millions of large determinants using a new method combining two systems of quadratic recurrence relations that have been around for two decades.[15, 36] This has never been tried before since the second work is not well-understood and its errata[36] has been published in an obscure place.

The first set of quadratic difference equations has been discovered by one of us[15] and for the symmetric case they reduce to

$$[C(m, n+1)\, C(m, n-1) - C(m, n)^2] + k[C^*(m+1, n)\, C^*(m-1, n) - C^*(m, n)^2] = 0 \tag{3.6}$$

$$[C(m+1, n)\, C(m-1, n) - C(m, n)^2] + k[C^*(m, n+1)\, C^*(m, n-1) - C^*(m, n)^2] = 0 \tag{3.7}$$

$$[C(m, n)\, C(m+1, n+1) - C(m+1, n)\, C(m, n+1)] = k[C^*(m, n)\, C^*(m+1, n+1) - C^*(m+1, n)\, C^*(m, n+1)] \tag{3.8}$$

$$\sqrt{k}[C(m+1, n)\, C^*(m-1, n) + C(m-1, n)\, C^*(m+1, n) + C(m, n+1)\, C^*(m, n-1) + C(m, n-1)\, C^*(m, n+1)] = (k+1)\, C(m, n)\, C^*(m, n) \tag{3.9}$$

where $C^*(m, n)$ is the dual (low-temperature) correlation function obtained by replacing $k \to 1/k$. Equations (3.6), (3.7), and (3.9) do not hold for $m = n = 0$ and

$$C(1, 0) = \sqrt{k+1} - \sqrt{k}\, C^*(0, 1), \qquad C(0, 1) = \sqrt{k+1} - \sqrt{k}\, C^*(1, 0) \tag{3.10}$$

is found in that case instead.

In order to apply these relations, it is necessary to have the diagonal correlation functions (with $m = n = N$). For the symmetric case we have

$$C(N, N+1) = C(N+1, N) \qquad \text{and} \qquad C^*(N, N+1) = C^*(N+1, N) \tag{3.11}$$

and these, together with all other pair correlation functions, can then be calculated recursively using (3.6)–(3.9). For $T = T_c$, we have the result known already to Onsager and Kaufman[4, 7, 10]

$$C(N, N) = C^*(N, N) = \prod_{j=1}^{N} \frac{\Gamma(j)^2}{\Gamma(j+1/2)\,\Gamma(j-1/2)} \tag{3.12}$$

For the general case, $T \neq T_c$, we have used the system of quadratic recurrence relations of Jimbo and Miwa[36] to be discussed in the following section.

4. DIAGONAL CORRELATIONS: TOEPLITZ DETERMINANTS AND QUADRATIC RECURRENCE RELATIONS

In this section we shall present the two ways we have used to calculate the diagonal correlation function.

4.1. Diagonal Correlations as Toeplitz Determinants

The first method derives from the fact that the diagonal correlations are given in terms of the Toeplitz determinants[7, 10]

$$\begin{aligned} \langle \sigma_{00} \sigma_{NN} \rangle &= \det{}_{1 \leqslant i,\, j \leqslant N} \{a_{i-j}\}, \\ \langle \sigma_{00} \sigma_{NN} \rangle^* &= \det{}_{1 \leqslant i,\, j \leqslant N} \{a^*_{i-j}\} \end{aligned} \tag{4.1}$$

with

$$a_n = \frac{1}{2\pi} \int_{-\pi}^{\pi} \mathrm{d}\theta \, \frac{k \cos n\theta - \cos(n+1)\,\theta}{\sqrt{1+k^2-2k\cos\theta}} \tag{4.2}$$

$$a_n^* = \frac{1}{2\pi} \int_{-\pi}^{\pi} \mathrm{d}\theta \, \frac{\cos n\theta - k \cos(n+1)\,\theta}{\sqrt{1+k^2-2k\cos\theta}} \tag{4.3}$$

Here the asterisk denotes the dual version with k replaced by $1/k$.

These elements have been expressed in terms of Legendre functions of the second kind[7, 32] or hypergeometric functions.[33] For numerical purposes it is more opportune to use recurrence relations. We believe that these linear recurrence relations will also provide the first step in giving an algebraic derivation of the system of quadratic recurrence relations discovered by Jimbo and Miwa[36] discussed in the next subsection and used in our numerical computations.

Defining the auxiliary quantities

$$b_n = \frac{1}{2\pi} \int_{-\pi}^{\pi} \mathrm{d}\theta \, \frac{\cos n\theta}{\sqrt{1+k^2-2k\cos\theta}} = b_{-n} \tag{4.4}$$

$$c_n = \frac{1}{2\pi} \int_{-\pi}^{\pi} \mathrm{d}\theta \cos n\theta \sqrt{1+k^2-2k\cos\theta} = c_{-n} \tag{4.5}$$

we have

$$a_n = kb_n - b_{n+1}, \quad \text{or} \quad a_{-n} = kb_n - b_{n-1}, \qquad \text{for} \quad T > T_c \tag{4.6}$$

and

$$a_n^* = b_n - kb_{n+1}, \quad \text{or} \quad a_{-n}^* = b_n - kb_{n-1}, \qquad \text{for} \quad T < T_c \tag{4.7}$$

Note that

$$a_n^* = -a_{-n-1}, \qquad a_n = -a_{-n-1}^* \tag{4.8}$$

so that the Toeplitz determinants for $T < T_c$ are also minors of the Toeplitz determinants for $T > T_c$ and vice versa. It may be noted that b_0 and c_0 are complete elliptic integrals of the first and second kind.

Since

$$(1+k^2-2k\cos\theta)\cos n\theta = (1+k^2)\cos n\theta - k\cos(n+1)\,\theta - k\cos(n-1)\,\theta \tag{4.9}$$

we have

$$c_n = (1+k^2)\, b_n - k b_{n+1} - k b_{n-1} \tag{4.10}$$

On the other hand, using partial integration,

$$c_n = -\frac{k}{2\pi n} \int_{-\pi}^{\pi} \mathrm{d}\theta \, \frac{\sin n\theta \sin\theta}{\sqrt{1+k^2-2k\cos\theta}} = \frac{k}{2n}\,(b_{n+1} - b_{n-1}) \tag{4.11}$$

These two equations imply

$$(2n-1)\, k b_{n-1} - 2n(1+k^2)\, b_n + (2n+1)\, k b_{n+1} = 0 \tag{4.12}$$

(It may be worth noting that for the row correlations this three-point relation is replaced by a similar five-point relation.)

We can also solve

$$(1-k^2)\, b_n = a_n^* - k a_n = k a_{n-1}^* - a_{n-1} \tag{4.13}$$

and find

$$(2n+1)\, a_n = 2nk^{-1} a_{n-1} - a_{n-1}^* = 2(n+1)\, k a_{n+1} + a_{n+1}^* \tag{4.14}$$

$$(2n+1)\, a_n^* = 2nk a_{n-1}^* - a_{n-1} = 2(n+1)\, k^{-1} a_{n+1}^* + a_{n+1} \tag{4.15}$$

or

$$(2n+1)\, a_n = 2nk^{-1} a_{n-1} - a_{-n} = 2(n+1)\, k a_{n+1} + a_{-n-2} \tag{4.16}$$

$$(2n+1)\, a_{-n-1} = 2nk a_{-n} - a_{n-1} = 2(n+1)\, k^{-1} a_{-n-2} + a_{n+1} \tag{4.17}$$

With these relations we can quickly calculate the elements of the Toeplitz determinants (4.1).

For the next-to-the-diagonal correlation function we have determinant expressions[16] like (4.1) but now with one row or column modified. These new elements satisfy similar recursion relations, which we shall present in a future publication. These results are needed when calculating or plotting correlation functions and q-dependent susceptibilities for nonsymmetric cases in which the absolute value of the coupling constants vary. We have done such calculations, but in this paper we will not present the details as our best results are based on the easier symmetric case.

4.2. Jimbo–Miwa Method

To calculate the diagonal Ising correlations, which are given above as Toeplitz determinants, turns out to be a nontrivial numerical problem. We

have found that in order to obtain accuracy of just ten significant figures in the final results, due to large cancellations, it is necessary to evaluate the elements of these determinants to high accuracy, as high as 250 digits, using a program like Maple. This is time and memory consuming even for today's powerful computers. Since we did such calculations, we have learnt from Dr. Nickel an efficient algorithm[53] to do these calculations.

However, there exists an even more efficient method for calculating the diagonal correlations using the recursion formulae of Miwa and Jimbo.[36] Then, for the symmetric case of the square Ising lattice with equal horizontal and vertical couplings, using the difference equations of the previous section we are able to obtain the correlations everywhere else, with distances between the spins up to several hundred lattice distances, in a matter of minutes on a desktop computer.

We make a slight change of notation with respect to Eq. (4) of ref. 36. The translation of the dependent variables is given by

$$\begin{aligned} &A_N=\sqrt{k'}\,\alpha_{-N}, \qquad B_N=\sqrt{k'}\,\beta_{-N}, \qquad C_N=-\sqrt{k'}\,\gamma_{-N},\\ &A_N^{\pm}=\sqrt{k'}\,\alpha_{-N}^{(\pm)}, \qquad B_N^{\pm}=\sqrt{k'}\,\beta_{-N}^{(\pm)}, \qquad C_N^{\pm}=-\sqrt{k'}\,\gamma_{-N}^{(\pm)},\\ &D_N^{\pm}=\sqrt{k'}\,\delta_{-N}^{(\pm)}, \qquad k'=\sqrt{1-k^2}, \qquad t=1/k^2 \end{aligned} \tag{4.18}$$

Then the diagonal correlation functions are given by Eq. (6) of ref. 36, i.e.,

$$A_N=C(N,N), \qquad C_N=C^*(N,N) \tag{4.19}$$

The three determinant conditions below Eq. (6) of ref. 36 become

$$A_{N-1}A_{N+1}+B_NC_N-A_N^2=0 \tag{4.20}$$

$$A_N^{\pm}D_N^{\pm}+B_N^{\pm}C_N^{\pm}-A_N^2=0 \tag{4.21}$$

The eight autonomous equations in Eq. (5) of ref. 36 are rewritten as

$$A_NA_{N+1}^{\pm}-A_{N+1}A_N^{\pm}+B_{N+1}C_{N+1}^{\pm}=0 \tag{4.22}$$

$$A_NB_{N+1}^{\pm}-k^{\pm 1}A_{N+1}B_N^{\pm}-B_{N+1}D_{N+1}^{\pm}=0 \tag{4.23}$$

$$k^{\pm 1}A_NC_{N+1}^{\pm}-A_{N+1}C_N^{\pm}+C_NA_N^{\pm}=0 \tag{4.24}$$

$$A_ND_{N+1}^{\pm}-A_{N+1}D_N^{\pm}-C_NB_N^{\pm}=0 \tag{4.25}$$

while the five non-autonomous equations become

$$(2N-1)\,A_{N+1}A_{N-1}-(2N+1)\,A_N^2+A_N^+D_N^++A_N^-D_N^-=0 \tag{4.26}$$

$$(2N+3)\,A_NB_{N+1}+kA_N^+B_N^++k^{-1}A_N^-B_N^-=0 \tag{4.27}$$

$$(2N+1)\,A_NC_{N+1}+C_{N+1}^+D_{N+1}^++C_{N+1}^-D_{N+1}^-=0 \tag{4.28}$$

$$(2N-1)\,A_{N+1}B_N+A_N^+B_N^++A_N^-B_N^-=0 \tag{4.29}$$

$$(2N+1)\,A_{N+1}C_N+kC_{N+1}^+D_{N+1}^++k^{-1}C_{N+1}^-D_{N+1}^-=0 \tag{4.30}$$

$$(2N-1)\,B_NC_N+B_N^+C_N^++B_N^-C_N^-=0 \tag{4.31}$$

Here the last equation (4.31) is new; it shows up as a condition when going through the details of the derivation in ref. 36; it is simpler than (4.26) from which it follows using (4.20) and (4.21).

Using Eq. (7) of ref. 36 the initial conditions are rewritten as

$$A_0=B_0=C_0=1,\qquad B_0^+=D_0^-=k',\qquad C_0^+=A_0^-=\frac{1}{k'},\qquad D_0^+=C_0^-=0,$$

$$A_1=\frac{2}{\pi}\,\mathrm{E}(k),\qquad A_0^+=\frac{2}{\pi k'}\,[2\mathrm{E}(k)-\mathrm{K}(k)],\qquad B_0^-=\frac{2k'}{\pi}\,[\mathrm{K}(k)-\mathrm{E}(k)] \tag{4.32}$$

where B_0^- is transcribed from the errata.[36]

The above equations are not all independent. Together with additional equations like (3.6)–(3.10), they form an overdetermined set of difference equations for the Ising model pair correlation function. Hence, the word "holonomic" in the title of ref. 36. We only need a subset of (4.20)–(4.32) to write an algorithm in order to obtain the initial conditions for (3.6)–(3.9).

In our Maple programs we have used the following eleven equations

$$B_{N+1}=-\frac{kA_N^+B_N^++k^{-1}A_N^-B_N^-}{(2N+3)\,A_N},$$

$$C_{N+1}^{\pm}=\frac{A_{N+1}C_N^{\pm}-C_NA_N^{\pm}}{k^{\pm1}A_N},\qquad D_{N+1}^{\pm}=\frac{A_{N+1}D_N^{\pm}+C_NB_N^{\pm}}{A_N},$$

$$C_{N+1}=-\frac{C_{N+1}^+D_{N+1}^++C_{N+1}^-D_{N+1}^-}{(2N+1)\,A_N}, \tag{4.33}$$

$$A_{N+1}^{\pm}=\frac{A_{N+1}A_N^{\pm}-B_{N+1}C_N^{\pm}}{A_N},\qquad B_{N+1}^{\pm}=\frac{k^{\pm1}A_{N+1}B_N^{\pm}+B_{N+1}D_N^{\pm}}{A_N},$$

$$A_{N+2}=\frac{A_{N+1}^2-B_{N+1}C_{N+1}}{A_N}$$

recursively.

The derivation in ref. 36 is terse and not easy to follow. No alternative derivation has ever been published. We have realized several of the above identities as Jacobi identities of Toeplitz determinants for A_N, B_N, C_N, and rewriting most of the other objects as similar determinants with one row or column modified. We hope to use this to show that Miwa–Jimbo type recursion formulae also exist for the correlations on the next-to-the diagonal row in the asymmetric case. But as all this work is incomplete for now, we shall not discuss it further.

Also, a reader who is uncomfortable with the derivation presented in ref. 36, should have no difficulty showing that the recurrence relations given above are correct. He can do this reproducing exactly the results from the Toeplitz determinants, analytically for shorter distances and numerically up to much larger distances.

5. FIBONACCI ISING MODEL WITH FERRO- AND ANTIFERROMAGNETIC BONDS OF EQUAL STRENGTH

So far we have discussed the correlation functions of the ferromagnetic Ising model on the square lattice with all interactions of equal strength. We can make interactions ferro- and antiferromagnetic according to Fibonacci rules using gauge transformations.

5.1. Definition of Fibonacci Ising model

We start by considering a two-dimensional square-lattice Ising model whose energy of interaction is defined by[3]

$$-\mathscr{E}/k_{\mathrm{B}}T=\sum_{i,\,j}\left[K_{i,\,j}\sigma_{i,\,j}\sigma_{i+1,\,j}+\bar{K}_{i,\,j}\sigma_{i,\,j}\sigma_{i,\,j+1}\right] \tag{5.1}$$

There are many possible ways of forming a Fibonacci Ising lattice. One of our choices is to let $K_{i,\,j}=K_i$ and $\bar{K}_{i,\,j}=\bar{K}_j$ and to choose either the K_i or the $\bar{K}_j$ or both to be Fibonacci sequences.

The infinite set of Fibonacci sequences $\{S_n\}$ is defined recursively by $S_{n+1}=S_nS_{n-1}$ with $S_0=\mathrm{B}$ and $S_1=\mathrm{A}$; then $S_2=\mathrm{AB}$, $S_3=\mathrm{ABA}$, $S_4=\mathrm{ABAAB}$ and so on. This uses symbols A and B that can represent many different things. The sequence S_n has F_n symbols with F_n the nth Fibonacci number given in (2.1).

[3] Here the $K_{i,\,j}$ represent the horizontal interactions and the $\bar{K}_{i,\,j}$ the vertical ones. In much of the literature[10] this is done the other way around.

The F_n-layered Ising model[39, 40, 51, 52] is formed by periodically repeating a unit cell of size F_n, such that inside each unit cell K_i (or $\bar{K}_j$) is either $K_{\mathbf{A}}$ or $K_{\mathbf{B}}$, depending upon whether the ith (or jth) position corresponds to an A or B in S_n. In the limit $F_n \to \infty$, it becomes an aperiodic Fibonacci Ising lattice. In this section we shall further restrict ourself to the case with $K_{\mathbf{A}} = -K$ and $K_{\mathbf{B}} = K$, where $K > 0$ so that the antiferromagnetic interactions are more abundant. It is well-known that the other case, $K_{\mathbf{A}} = K$ and $K_{\mathbf{B}} = -K$, follows by flipping the sign of each second spin, which will only lead to a shift $q_x \to q_x \pm \pi$ and/or $q_y \to q_y \pm \pi$ in the $\chi(q_x, q_y)$.

Unlike the model studied by Tracy,[39] the critical temperature and free energy in these cases are identical to the ones in the ferromagnetic case. This can be easily seen as follows. Let $N(i)$ denote the number of negative bonds among $\{K_1, K_2, ..., K_{i-1}\}$ and $\bar{N}(j)$ the number of negative bonds among $\{\bar{K}_1, \bar{K}_2, ..., \bar{K}_{j-1}\}$. Then we can define the gauge transformation

$$\sigma_{i,j} \to (-1)^{N(i)+\bar{N}(j)} \sigma_{i,j} \tag{5.2}$$

The partition function, which is a sum over all the spin variables, is invariant under such spin flips and the resulting sum equals the partition function of the ferromagnetic model. Consequently, the free energy is invariant.

5.2. Fibonacci in Both Horizontal and Vertical Directions

However, the connected pair correlation function is easily seen to pick up signs, i.e.,

$$\langle \sigma_{i_1,j_1} \sigma_{i_2,j_2} \rangle^{(c)} \to (-1)^{N(i_1)+\bar{N}(j_1)+N(i_2)+\bar{N}(j_2)} \langle \sigma_{i_1,j_1} \sigma_{i_2,j_2} \rangle_0^{(c)} \tag{5.3}$$

where $\langle \sigma_{i_1,j_1} \sigma_{i_2,j_2} \rangle_0$ is the correlation function in the regular ferromagnetic square Ising model and the superscript (c) is used to indicate that we are having connected two-point correlation functions given by

$$\langle \sigma_{i_1,j_1} \sigma_{i_2,j_2} \rangle^{(c)} = \langle \sigma_{i_1,j_1} \sigma_{i_2,j_2} \rangle - \langle \sigma_{i_1,j_1} \rangle \langle \sigma_{i_2,j_2} \rangle \tag{5.4}$$

Hence, due to these sign factors in the F_n-layered Fibonacci Ising model, the q-dependent susceptibility defined by

$$k_{\mathbf{B}} T \chi(q_x, q_y) = \lim_{\mathscr{L} \to \infty} \frac{1}{\mathscr{L}^2} \sum_{l_1, m_1} \sum_{l_2, m_2} e^{i[q_x(l_2 - l_1) + q_y(m_2 - m_1)]} \langle \sigma_{l_1, m_1} \sigma_{l_2, m_2} \rangle^{(c)} \tag{5.5}$$

where $\mathscr{L} = LF_n$ is both the number of rows and columns in the lattice, with L denoting some positive integer, is different from that in the ferromagnetic case. We may rewrite

$$k_{\mathrm{B}} T\chi(q_x, q_y) = \sum_{l,\, m = -\infty}^{\infty} \mathrm{e}^{\mathrm{i}(q_x l + q_y m)} C^{(\mathrm{c})}(l, m) \tag{5.6}$$

where

$$C^{(\mathrm{c})}(l, m) = \lim_{\mathscr{L} \to \infty} \frac{1}{F_n^2} \sum_{l',\, m' = 0}^{F_n - 1} \langle \sigma_{l', m'} \sigma_{l + l', m + m'} \rangle^{(\mathrm{c})} \tag{5.7}$$

averaging over the unit cell.

We can simplify this using a result obtained by Tracy.[39] We let $N(m, m')$ be the number of negative horizontal bonds (or A's in the Fibonacci sequence) among the m bonds sandwiched between the m'th and $(m' + m)$th columns. Using Lemma 2.5 in ref. 39, we find that $N(m, m')$ is either $\lfloor N_m \rfloor$ or $\lfloor N_m \rfloor + 1$, where $N_m = mF_{n-1}/F_n$ and $\lfloor x \rfloor$ denotes the integer part of x. Furthermore, in the interval $0 \leqslant m' \leqslant F_n - 1$, the number of times that $N(m, m')$ equals $\lfloor N_m \rfloor$ is $F_n(1 - \{N_m\})$, where $\{x\}$ is the fractional part of x, while the number of times that $N(m, m')$ equals $\lfloor N_m \rfloor + 1$ is $F_n\{N_m\}$. A similar relation holds for the vertical bonds. Consequently, we find from (5.3) and (5.7) that

$$C^{(\mathrm{c})}(l, m) = \phi_n(l)\, \phi_n(m) \langle \sigma_{0,0} \sigma_{l, m} \rangle_0^{(\mathrm{c})} = \phi_n(l)\, \phi_n(m)\, C_0^{(\mathrm{c})}(l, m) \tag{5.8}$$

where the averaged phase factor is

$$\begin{aligned} \phi_n(m) &= (-1)^{\lfloor N_m \rfloor} (1 - \{N_m\}) + (-1)^{\lfloor N_m \rfloor + 1} \{N_m\} \\ &= (-1)^{\lfloor m\alpha_n \rfloor} (1 - 2\{m\alpha_n\}), \qquad \alpha_n \equiv F_{n-1}/F_n \end{aligned} \tag{5.9}$$

and $C_0^{(\mathrm{c})}(l, m)$ is readily calculated using the methods of Sections 3 and 4.

Using the simple relation $\lfloor x \rfloor = x - \{x\}$, we may rewrite

$$\phi_n(m) = \mathrm{e}^{\pi \mathrm{i} m \alpha_n} \psi(m\alpha_n), \qquad \text{with} \quad \psi(x) \equiv \mathrm{e}^{-\pi \mathrm{i}\{x\}} (1 - 2\{x\}) \tag{5.10}$$

Then, as $\psi(x)$ is a periodic continuous function of period 1, it is easy to show that it has the Fourier series

$$\psi(x) = \sum_{p = -\infty}^{\infty} \frac{\mathrm{e}^{2\pi \mathrm{i} p x}}{(p + 1/2)^2 \pi^2} \tag{5.11}$$

Next, writing $p = jF_n + l$ for $-\infty < j < \infty$ and $0 \leqslant l \leqslant F_n - 1$, and noting that $jF_n m\alpha_n$ is an integer, we find

$$\phi_n(m) = \sum_{l=0}^{F_n-1} e^{2\pi i(l+1/2)\alpha_n m} \hat{\phi}_n(l) \tag{5.12}$$

$$\hat{\phi}_n(l) \equiv \sum_{j=-\infty}^{\infty} \frac{1}{(jF_n + l + 1/2)^2 \pi^2} = \hat{\phi}_n(F_n - 1 - l) \tag{5.13}$$

Substituting (5.8) into (5.6) and then using (5.12), we find

$$\chi(q_x, q_y) = \sum_{l=0}^{F_n-1} \sum_{m=0}^{F_n-1} \hat{\phi}_n(l)\, \hat{\phi}_n(m) \times \chi_0(q_x + 2\pi\alpha_n(l+1/2),\, q_y + 2\pi\alpha_n(m+1/2)) \tag{5.14}$$

where χ_0 denotes the q-dependent susceptibility of the ferromagnetic uniform two-dimensional Ising model and its maximum is at $q_x = q_y = 0$ and for $T \to T_c$ this diverges as[11, 31]

$$\chi_0(0, 0) \approx c_{\pm} |t|^{-7/4}, \qquad t = \frac{T}{T_c} - 1 \propto 1 - k \tag{5.15}$$

Therefore, there should be $F_n \times F_n$ peaks located at $q_x = 2\pi\alpha_n(l + 1/2)$ and $q_y = 2\pi\alpha_n(m + 1/2) \bmod 2\pi$, for $0 \leqslant l,\ m \leqslant F_n - 1$. The predominant peaks are seen to be at $l = m = 0$ and $l = m = F_n - 1$, or $q_x, q_y = \pm\pi\alpha_n \pmod{2\pi}$.

5.3. Aperiodic in Both Horizontal and Vertical Directions

In the limit $n \to \infty$ we have $F_{n-1}/F_n \to \alpha$, with α being the golden ratio, which is an irrational number. Then the effective connected correlation function (5.9) tends to

$$C^{(c)}(l, m) = \phi(l)\, \phi(m) \langle \sigma_{0,0} \sigma_{l,m} \rangle_0^{(c)} = \phi(l)\, \phi(m)\, C_0^{(c)}(l, m) \tag{5.16}$$

where the averaged phase factor (5.9) becomes

$$\phi(m) = \phi_\infty(m) = (-1)^{\lfloor m\alpha \rfloor} (1 - 2\{m\alpha\}), \qquad \alpha \equiv \tfrac{1}{2}(\sqrt{5} - 1) \tag{5.17}$$

Also, $F_n \to \infty$ and it is easy to see that only $j = 0$ and $j = -1$ in the sum (5.13) contribute, so that we now have

$$\phi(m) = \sum_{l=-\infty}^{\infty} \frac{e^{2\pi i(l+1/2)\alpha m}}{(l+1/2)^2 \pi^2} = \phi(-m) \tag{5.18}$$

in this limit (with $l \geqslant 0$ from $j=0$ and $l<0$ from $j=-1$). This can, of course, also be derived directly from (5.17).

Therefore, in this aperiodic limit, the q-dependent susceptibility becomes

$$\chi(q_x, q_y) = \sum_{l=-\infty}^{\infty} \sum_{m=-\infty}^{\infty} \frac{\chi_0(q_x + 2\pi\alpha(l+1/2),\, q_y + 2\pi\alpha(m+1/2))}{(l+1/2)^2\,(m+1/2)^2\,\pi^4} \tag{5.19}$$

which shows that it is made up from an infinite number of peaks densely located in the square with q_x and q_y between 0 and 2π. For T away from T_c, the correlation length is finite and due to overlap only a finite number of peaks will be observed. It may also be remarked that, because of the identity

$$\sum_{l=-\infty}^{\infty} \frac{1}{(l+1/2)^2\,\pi^2} = 1 \tag{5.20}$$

the integrals of $\chi(q_x, q_y)$ and $\chi_0(q_x, q_y)$ for q_x, q_y from 0 to 2π are the same and, in fact, they both equal $(2\pi)^2/(k_B T)$ as they both are proportional to the autocorrelation $\langle \sigma_{i,j}^2 \rangle = 1$.

For all models in this section, obtained by gauge transformations adding signs, the row (and column) correlation length ξ is the same at the same given elliptic modulus k. Above T_c it is given by[2, 8–10]

$$\xi^{-1} = \xi_>^{-1}(k) = |2K - 2K^*| = |\operatorname{arsinh}(k^{1/2}) - \operatorname{arsinh}(k^{-1/2})| \tag{5.21}$$

whereas below T_c, at $k>1$, it is precisely one half[8–10] of the above T_c value at $k \to 1/k$, i.e., $\xi_<(k) = \frac{1}{2}\xi_>(1/k)$. This difference will also manifest itself in the following.

First, we plot the q-dependent susceptibility $\chi_0(q_x, q_x)$ of the uniform symmetric ferromagnetic Ising model. It is shown in Fig. 1 for three different values of the correlation length, $\xi = 1$, 2 and 3. It has a single peak at $q_x = q_y = 0$, which becomes less tall and more broadened as T moves away from T_c. This gives rise to a larger contribution to the background, explaining why all but a few peaks are suppressed in the different Fibonacci cases.

Next, we make plots for the $n=4$ and $n=\infty$ Fibonacci Ising models. We do this by calculating the Fourier sums (5.6) using (5.8) and algorithms based on Sections 3 and 4. Since the correlation functions decay exponentially, only a finite number of terms in (5.6) is significant. For $\xi < 3$, there are only four peaks in a unit cell of the reciprocal lattice, which are all symmetrically located on the lines $q_x = \pm q_y \pmod{2\pi}$. We plot one of these peaks of $\chi(q_x, q_x)$ for $\xi = 1, 2, 3$ in Fig. 2. Figure 2a is for the periodic layered case with period $F_4 = 5$. According to (5.14) the location of the

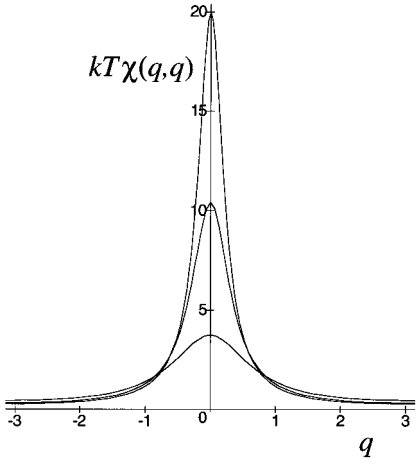

Fig. 1. The reduced q-dependent susceptibility of the ferromagnetic Ising model $k_B T\chi_0(q_x, q_x)$ is plotted versus $q = q_x = q_y$ for $\xi = 1, 2, 3$ and $T > T_c$. Its peak at $q = 0$ becomes more sharp as ξ increases.

peak of the q-dependent susceptibility should approach $q_x = \alpha_4 \pi = 3\pi/5 = 1.8850$ as ξ increases. Figure 2b is for the aperiodic case, for which the peak approaches the limiting position $q_x = \alpha\pi = 1.9416$ in agreement with (5.19). Thus, the peaks approach different positions for the two cases, one commensurate and the other incommensurate.

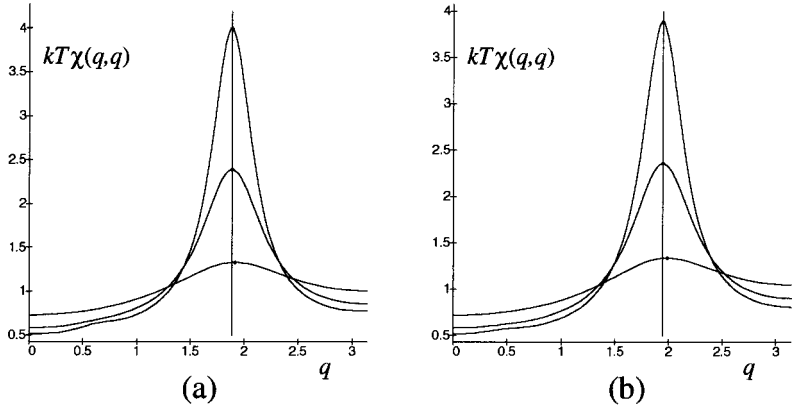

Fig. 2. The reduced q-dependent susceptibilities $k_B T\chi(q_x, q_x)$ of (a) the F_4-periodic and (b) the aperiodic Fibonacci Ising models are plotted versus $q = q_x = q_y$ for $\xi = 1, 2, 3$ and $T > T_c$. As ξ increases, the peaks approach (a) the commensurate position $3\pi/5$ for the periodic case with $F_4 = 5$ and (b) the incommensurate position $\alpha\pi$ for the aperiodic case.

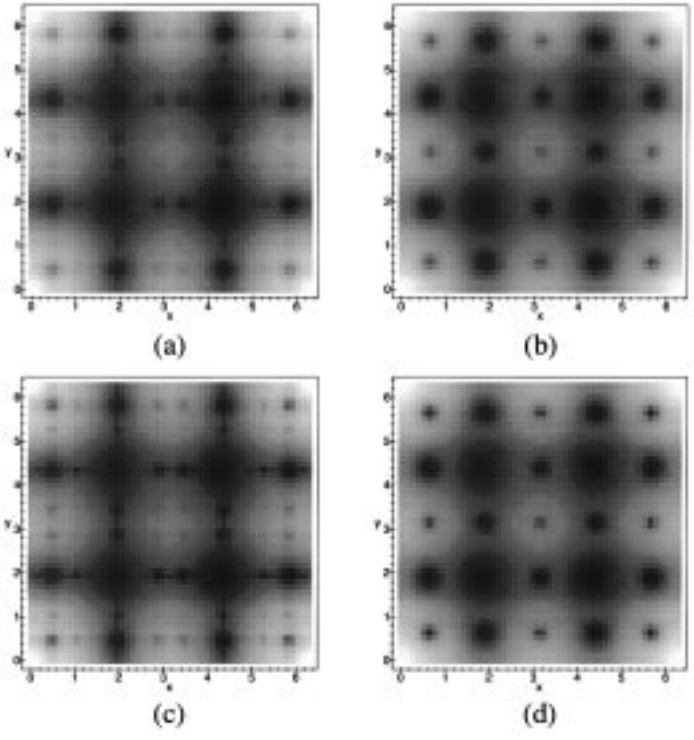

Fig. 3. Density plots of the q-dependent susceptibility for $T > T_c$: Here $\chi(q_x, q_y)$ for the aperiodic case with $\xi = 8$ corresponding to $k = 0.8379$ is shown in (a) and the periodic case with $F_4 = 5$ and again $\xi = 8$ is shown in (b). Below each figure are shown density plots for a different temperature corresponding to $\xi = 16$ and $k = 0.9154$ in (c) and (d). Note that the periodic cases (b) and (d) have exactly 25 peaks regularly spaced.

Moreover, as $\xi \to \infty$ there is an ever-increasing number of peaks for the aperiodic case, as can be seen from (5.19), whereas there is a maximum number of peaks in the periodic case, namely F_n^2 according to (5.14). This is illustrated in Fig. 3, where we give four density plots of the q-dependent susceptibilities, two for the F_4-layered case with $F_4 = 5$ and two for the aperiodic case. We have chosen $T > T_c$ and $\xi = 8$ for the top figures and $\xi = 16$ for the bottom ones.

Each plot has the square q_x, q_y from 0 to 2π subdivided into 50×50 little squares, where a darker texture indicates a larger value of $\chi(q_x, q_y)$.[4]

[4] All our density plots were prepared plotting $1/\chi(q_x, q_y)$ using Maple V release 4. This is done in order to bring out the subdominant peaks.

The figures for the periodic case on the right show that the number of peaks for $\xi = 8$ equals the number of peaks for $\xi = 16$, both numbers equalling $F_4^2 = 25$. In the left two plots, we show that for the aperiodic lattice there are more peaks than in the periodic case and their number is increased when the correlation length is doubled. We see that the periodic and aperiodic cases are quite different, unless the size of the unit cell F_n is fairly large, so that (5.14) and (5.19) are hard to distinguish numerically. Therefore, the point raised in Section 2.1 is a valid one.

Next, in order to study the point brought up in Section 2.2, we have to compare results for ordered and disordered states. For this purpose, we have given density plots of the q-dependent susceptibility for the aperiodic Fibonacci Ising model for $T > T_c$ in Fig. 4 and for $T < T_c$ in Fig. 5. We find that there are more peaks in the q-dependent susceptibility for $T > T_c$ than for $T < T_c$, when comparing Fig. 4 and Fig. 5. This is a consequence of the

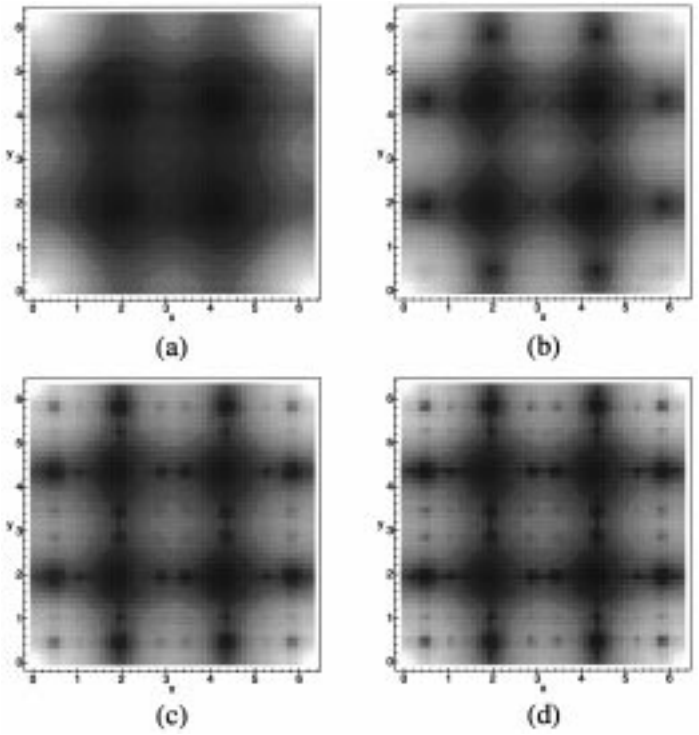

Fig. 4. Density plots of $\chi(q_x, q_y)$ for $T > T_c$ for a lattice with aperiodicity in both the horizontal and vertical directions: (a) $\xi = 1$ corresponding to $k = 0.2364$; (b) $\xi = 4$ or $k = 0.7019$; (c) $\xi = 12$ or $k = 0.8888$; and (d) $\xi = 20$ or $k = 0.9317$.

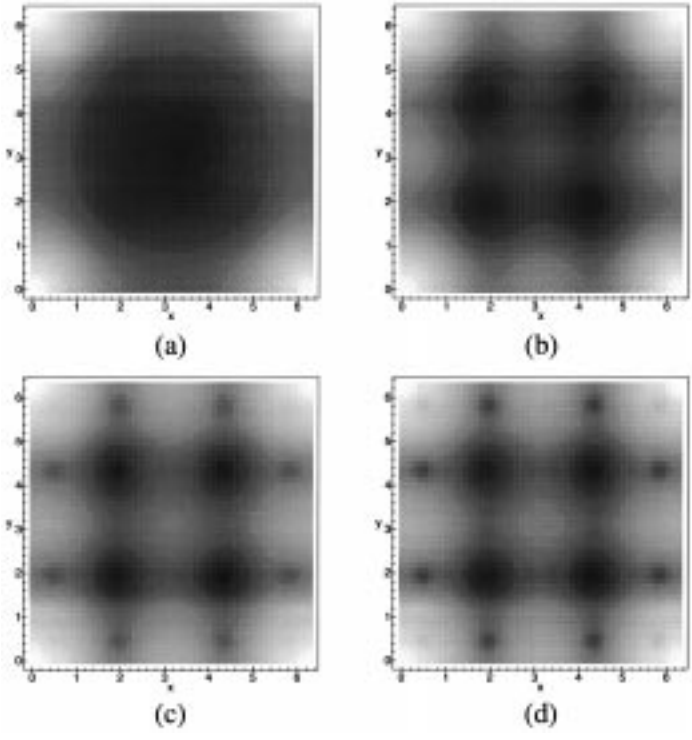

Fig. 5. Density plots of $\chi(q_x, q_y)$ for $T < T_c$ for a lattice with aperiodicity in both the horizontal and vertical directions: (a) $\xi = \frac{1}{2}$ corresponding to $k = 4.2309$; (b) $\xi = 2$ or $k = 1.4248$; (c) $\xi = 6$ or $k = 1.1251$; and (d) $\xi = 10$ or $k = 1.0733$. These parameters follow from the dual parameters of Fig. 4 by the replacements $k \to 1/k$ and $\xi \to \frac{1}{2}\xi$. In the Ising model, there are no "single-particle excitations" for $T < T_c$, explaining the twice faster exponential decay of the connected correlations.

well-known fact[8–10] that the connected correlation function for $T < T_c$ decays with the correlation length $\frac{1}{2}\xi$, with ξ the correlation length of the dual temperature above T_c, see also the discussion below (5.21). Using the methods of Sections 3 and 4 it is natural to generate the pair correlation functions for dual pairs of temperatures corresponding to pairs k and $1/k$, and this is what we have done to generate the two sets of plots.

We conclude from our results that the disordered and the ordered states can both exhibit the everywhere dense and incommensurate peaks in the wavevector-dependent susceptibility. We have even verified that the plots of these two cases are fairly similar, provided the correlation lengths coincide. Therefore, we shall only show $T > T_c$ plots in the following.

5.4. Aperiodic Only in the Horizontal Direction

If the model is aperiodic only in the horizontal direction, we must replace (5.16) by

$$C^{(c)}(l, m) = \phi(l) \langle \sigma_{0,0} \sigma_{l,m} \rangle_0^{(c)} = \phi(l)\, C_0^{(c)}(l, m) \tag{5.22}$$

with $\phi(l)$ still given by (5.17) and (5.18). Instead of (5.19) we now have

$$\chi(q_x, q_y) = \sum_{l=-\infty}^{\infty} \frac{\chi_0(q_x + 2\pi\alpha(l+1/2), q_y)}{(l+1/2)^2 \pi^2} \tag{5.23}$$

which shows that $\chi(q_x, q_y)$ has peaks on the q_x axis.

The density plot of the q-dependent susceptibility for $T > T_c$ is given in Fig. 6 for different values of the correlation length. This is again done by

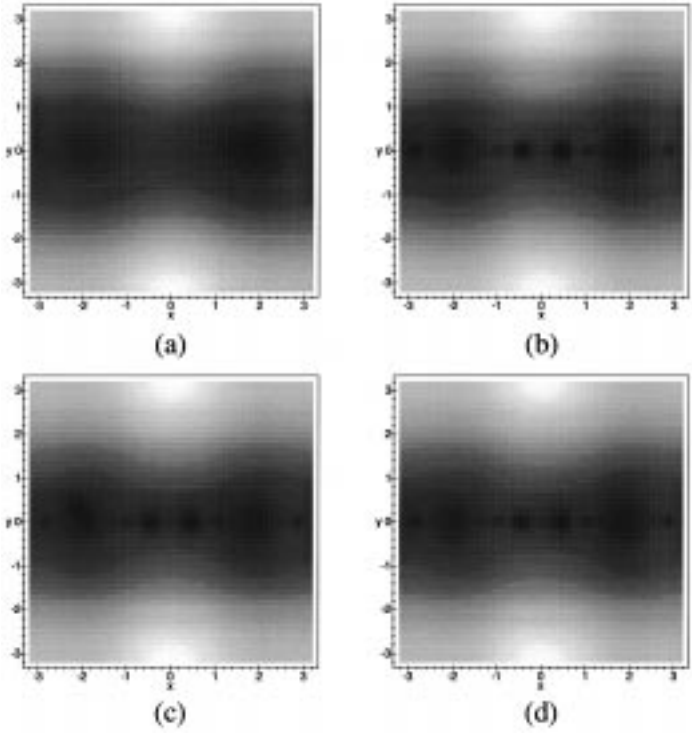

Fig. 6. Density plots of $\chi(q_x, q_y)$ for $T > T_c$ for a lattice with aperiodicity in the horizontal direction only. (a) $\xi = 1$ corresponding to $k = 0.2364$; (b) $\xi = 4$ or $k = 0.7019$; (c) $\xi = 12$ or $k = 0.8888$; and (d) $\xi = 20$ or $k = 0.9317$.

calculating a truncated sum (5.6), but now using (5.22). We indeed find that the peaks become more and more dense on the line $q_y = 0$.

5.5. Aperiodic in One Diagonal Direction

If the model is aperiodic only in one diagonal direction, we choose the sign of the bonds the same in each (anti)diagonal staircase. It is not hard to see that we must now replace (5.16) by

$$C^{(c)}(l, m) = \phi(l+m)\langle \sigma_{0,0}\sigma_{l,m}\rangle_0^{(c)} = \phi(l+m)\, C_0^{(c)}(l, m) \tag{5.24}$$

with $\phi(l)$ again given by (5.17) and (5.18). Instead of (5.19) we find

$$\chi(q_x, q_y) = \sum_{l=-\infty}^{\infty} \frac{\chi_0(q_x + 2\pi\alpha(l+1/2),\, q_y + 2\pi\alpha(l+1/2))}{(l+1/2)^2\,\pi^2} \tag{5.25}$$

which shows that $\chi(q_x, q_y)$ has peaks on the $q_x = q_y$ diagonal.

The density plot of the q-dependent susceptibility for $T > T_c$ is given in Fig. 7 for different values of the correlation length. This is again done by calculating a truncated sum (5.6), but now using (5.24). We indeed find that the peaks become more and more dense on the line $q_x = q_y$.

5.6. Aperiodic in Both Diagonal Directions

If the model is aperiodic in both of the diagonal directions, we must replace (5.16) by

$$C^{(c)}(l, m) = \phi(l+m)\,\phi(l-m)\, C_0^{(c)}(l, m) \tag{5.26}$$

with $\phi(l)$ still given by (5.17) and (5.18). Instead of (5.19) we can derive

$$\chi(q_x, q_y) = \sum_{l=-\infty}^{\infty} \sum_{m=-\infty}^{\infty} \frac{\chi_0(q_x + 2\pi\alpha(l+m+1),\, q_y + 2\pi\alpha(l-m))}{(l+1/2)^2\,(m+1/2)^2\,\pi^4} \tag{5.27}$$

This looks asymmetric at first sight, but the simple replacement $m \to -m-1$ shows that indeed $\chi(q_x, q_y) = \chi(q_y, q_x)$. Equation (5.27) proves that $\chi(q_x, q_y)$ has peaks which become everywhere dense as $T \to T_c$.

The density plot of the q-dependent susceptibility for $T > T_c$ is given in Fig. 8 for different values of the correlation length. This is also done by calculating a truncated sum (5.6), but now using (5.26). This case gives the most spectacular plots with incommensurate peaks that become more and

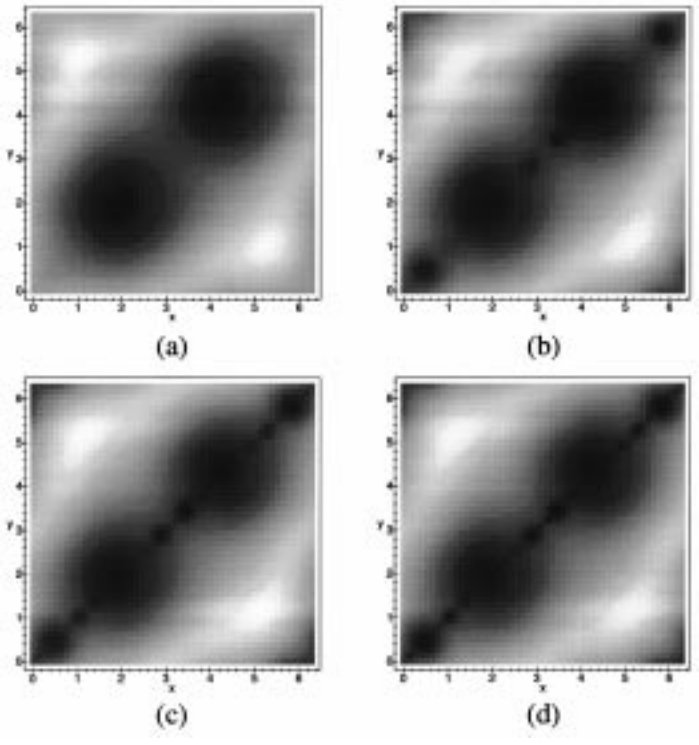

Fig. 7. Density plots of $\chi(q_x, q_y)$ for $T > T_c$ for a lattice with aperiodicity in one of the diagonal directions only. (a) $\xi = 1$ corresponding to $k = 0.2364$; (b) $\xi = 4$ or $k = 0.7019$; (c) $\xi = 12$ or $k = 0.8888$; and (d) $\xi = 20$ or $k = 0.9317$.

more dense in the plane, showing that the number of peaks is related to the correlation length.

6. SCALING LIMIT FOR TWO-POINT CORRELATION FUNCTION IN *Z*-INVARIANT ISING MODEL

In this section we shall derive a new result for the two-point correlation function of the Z-invariant Ising model in the scaling limit.

6.1. *Z*-Invariant Ising Model

The Z-invariant inhomogeneous Ising model[12, 13] has been introduced by Baxter as a natural extension of Onsager's uniform Ising model within the framework of star-triangle equations and commuting transfer matrices. It is defined in terms of a set of oriented straight lines carrying

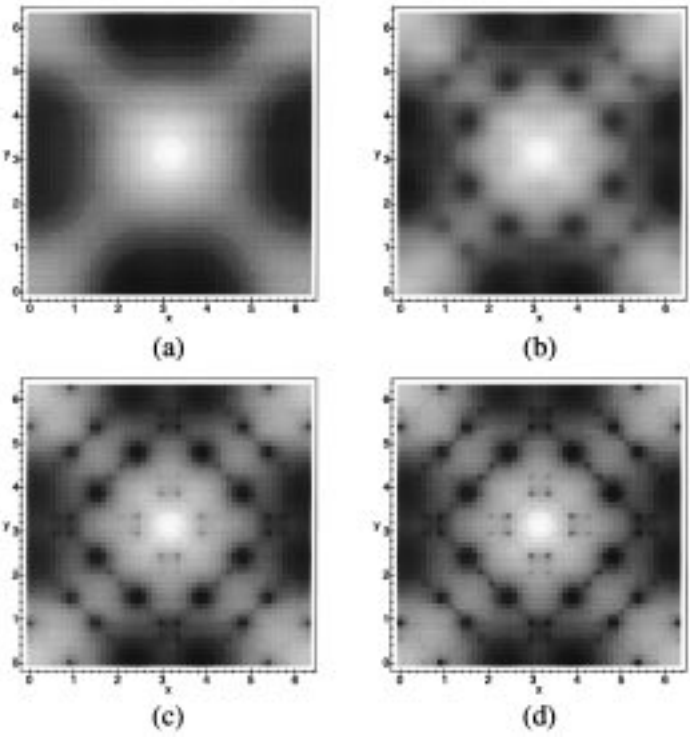

Fig. 8. Density plots of $\chi(q_x, q_y)$ for $T > T_c$ for a lattice with aperiodicity in both diagonal directions. (a) $\xi = 1$ corresponding to $k = 0.2364$; (b) $\xi = 4$ or $k = 0.7019$; (c) $\xi = 12$ or $k = 0.8888$; and (d) $\xi = 20$ or $k = 0.9317$.

"rapidity" variables u_i. Only two lines can meet at each intersection and the areas separated by the rapidity lines can be colored alternatingly black and white. An Ising spin is associated with each black area and a dual Ising spin with each white area, see also Fig. 9.

This defines two Ising models. In the first one each pair of spins meeting at an intersection of two rapidity lines has the usual pair interaction $-K\sigma_x\sigma_y$ with reduced interaction strength $K = \beta J$. In the second model the two dual spins that meet at the same intersection interact as $-K^*\sigma_{x^*}\sigma_{y^*}$, where $\sinh(2K)\sinh(2K^*) = 1$. Here K and therefore also K^* only depend on a fixed elliptic modulus k and the two rapidity variable u_1 and u_2 of the two rapidity lines that meet.

We have two possible choices for the reduced interaction strength $K_{x,y}$ of the spins at positions x and y, see Fig. 10. If the two rapidity lines with rapidity variables u_1 and u_2 pass through the line connecting the two spins

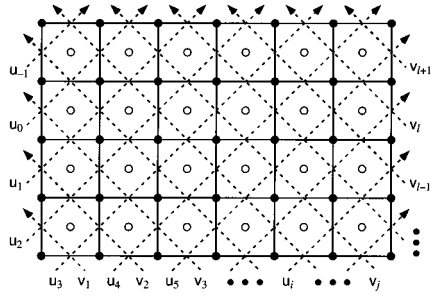

Fig. 9. The lattice of a two-dimensional Z-invariant Ising model is represented by solid lines, the rapidity lines on the medial graph are represented by oriented dashed lines. These lines carry rapidity variables u_i and v_j. The position of the spins are indicated by small black circles, the positions of the dual spins by white circles.

toward the same side of that line, we must choose $K_{x,\,y} = K(u_1, u_2)$; otherwise, if they pass toward opposite sides, we must take $K_{x,\,y} = \bar{K}(u_1, u_2)$. These choices $K(u_1, u_2)$ and $\bar{K}(u_1, u_2)$ are given by

$$\begin{aligned} \sinh(2K(u_1, u_2)) &= k\,\mathrm{sc}(u_1 - u_2, k') = \mathrm{cs}(\mathrm{K}(k') + u_2 - u_1, k'), \\ \sinh(2\bar{K}(u_1, u_2)) &= \mathrm{cs}(u_1 - u_2, k') = k\,\mathrm{sc}(\mathrm{K}(k') + u_2 - u_1, k') \end{aligned} \tag{6.1}$$

where $k' = \sqrt{1 - k^2}$ is the complementary elliptic modulus, $\mathrm{K}(k)$ denotes the complete elliptic integral of the first kind, and $\mathrm{sc}(v, k) = \mathrm{sn}(v, k)/\mathrm{cn}(v, k)$ and $\mathrm{cs}(v, k) = \mathrm{cn}(v, k)/\mathrm{sn}(v, k)$ are Jacobi elliptic functions. There is still a sign ambiguity in (6.1) depending on which of the two rapidity lines carries u_1 and which u_2. This ambiguity is removed if we take u_1 to be the rapidity variable of the line that points in a direction (less than 180°) clockwise with respect to the other rapidity line. [In Fig. 10 we have to identify u_i as the u_1 and v_j as the u_2 of (6.1).]

Equation (6.1) also exhibits a remarkable "rotation symmetry" in this Z-invariant Ising model. We can flip the direction of a rapidity line j providing we change its rapidity variable u_j to $u_j \pm \mathrm{K}(k')$. This interchanges

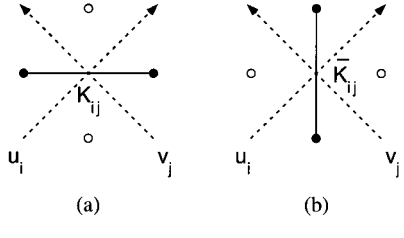

Fig. 10. (a) The horizontal coupling K_{ij} and (b) the vertical coupling $\bar{K}_{ij}$.

the K and $\bar{K}$ choices in (6.1). It is a simple exercise to see that this is consistent using $\mathrm{sc}(v+2\mathrm{K}(k'),k')=\mathrm{sc}(v,k')$ and the corresponding periodicity formula for $\mathrm{cs}(v,k')=1/\mathrm{sc}(v,k')$. This symmetry plays an important role in the calculation of the correlation functions and was noted before. We shall now exploit it.

In the Z-invariant Ising model, following Baxter's argument,[12, 13] the two-point correlation function can only depend on the elliptic modulus k and the values of the $2m$ rapidity variables $u_1,...,u_{2m}$ that pass between the two spins under consideration. Hence, there should exist universal functions $g_2,...,g_{2m}$ such that for the appropriate m-value

$$\langle \sigma\sigma' \rangle = g_{2m}(k;\bar{u}_1,...,\bar{u}_{2m}) = g_{2m}(k;\bar{u}_{\mathrm{P}(1)}+v,...,\bar{u}_{\mathrm{P}(2m)}+v) \tag{6.2}$$

where $\bar{u}_j=u_j$ if the jth rapidity line passes between the two spins σ and σ' in a fixed chosen direction and[16] $\bar{u}_j=u_j+\mathrm{K}(k')$ if it passes in the opposite direction. The Z-invariance implies that there should be complete permutation symmetry under all permutations P of the rapidities and the "difference property" implies a translation invariance when shifting all the u_j by the same amount v. These properties have been expressed in the above equation.

If two rapidity variables differ by $\mathrm{K}(k')$, they can be viewed as belonging to a single rapidity line passing between the two spins and back. The correlation function cannot depend on them, i.e.,

$$\begin{aligned}\langle \sigma\sigma' \rangle &= g_{2m+2}(k;\bar{u}_1,...,\bar{u}_{2m},\bar{u}_{2m+1},\bar{u}_{2m+1}+\mathrm{K}(k')) \\ &= g_{2m}(k;\bar{u}_1,...,\bar{u}_{2m})\end{aligned} \tag{6.3}$$

6.2. Scaling Limit

We can use these properties (6.2) and (6.3) to propose a formula for the two-point function in the scaling limit, where $k\to 1$ and the distance of the spins tends to infinity. In this limit we have $\mathrm{K}(k')=\frac{1}{2}\pi$,

$$\sinh(2K(u_1,u_2)) = \tan(u_1-u_2) = \cot(\pm\tfrac{1}{2}\pi+u_2-u_1) \tag{6.4}$$

$$\sinh(2\bar{K}(u_1,u_2)) = \cot(u_1-u_2) = \tan(\pm\tfrac{1}{2}\pi+u_2-u_1) \tag{6.5}$$

The scaling limit is defined by the assumption that the scaled correlation function depends on a single distance variable R. We can view the rapidity variables as angle variables, and the translation symmetry in (6.3) becomes a rotation symmetry in a two-dimensional plane. Writing the u_j in terms

of unit vectors $\mathbf{e}_j = (\cos(\lambda u_j), \sin(\lambda u_j))$, the simplest expression for R that exhibits the required rotation and permutation symmetries is

$$R = C \left| \sum_{j=1}^{2m} \mathbf{e}_j \right| \qquad \text{or} \quad R = \frac{1}{2} \left[\left\{ \sum_{j=1}^{2m} \cos(2u_j) \right\}^2 + \left\{ \sum_{j=1}^{2m} \sin(2u_j) \right\}^2 \right]^{1/2} \tag{6.6}$$

We can only have $\lambda = 2$ in view of (6.3) which says that any pair u and $u + \frac{1}{2}\pi$ must cancel out.[5] It appears that the only freedom available is the scale factor C which we can choose to be $C = \frac{1}{2}$.

For the special case of diagonal correlations $\langle \sigma_{00} \sigma_{mm} \rangle$ in the uniform rectangular Ising model, for which all $2m$ u_j's are equal, we find from (6.6) $R = m$, justifying the above choice of C. In this special case the correlation length ξ_d is known[10] and we can use it to introduce the scaled distance[6]

$$r = R/\xi_d, \qquad \text{where} \quad \xi_d^{-1} = |\log k| \tag{6.7}$$

We can now propose the general form of the scaled correlation functions to be

$$\langle \sigma\sigma' \rangle \approx |1 - k^{-2}|^{1/4} F(r), \qquad \langle \sigma\sigma' \rangle^* \approx |1 - k^{-2}|^{1/4} G(r) \tag{6.8}$$

where the functions $F(r)$ and $G(r)$ are expected to be Painlevé functions and the front factor is the square of the spontaneous magnetization for $T < T_c$ or $k > 1$.

We leave it as an exercise to the reader to verify that these scaling forms agree with all existing results for the uniform rectangular and triangular Ising models.[11, 35] Some details will be presented in the next section. We shall proceed with providing strong evidence that they are also correct for the general Z-invariant Ising model.

For the most general planar Ising model we can use a quadratic identity relating the two-point correlation function $\langle \sigma_x \sigma_y \rangle$ with its counterpart on the dual lattice $\langle \sigma_{x^*} \sigma_{y^*} \rangle^*$, i.e.,[15]

$$\begin{aligned} &\sinh(2K_1) \sinh(2K_2) \{ \langle \sigma_{x_1} \sigma_{x_2} \rangle \langle \sigma_{y_1} \sigma_{y_2} \rangle - \langle \sigma_{x_1} \sigma_{y_2} \rangle \langle \sigma_{y_1} \sigma_{x_2} \rangle \} \\ &\quad + \{ \langle \sigma_{x_1^*} \sigma_{x_2^*} \rangle^* \langle \sigma_{y_1^*} \sigma_{y_2^*} \rangle^* - \langle \sigma_{x_1^*} \sigma_{y_2^*} \rangle^* \langle \sigma_{y_1^*} \sigma_{x_2^*} \rangle^* \} = 0 \end{aligned} \tag{6.9}$$

[5] Consistency with the symmetry related to the flipping of the direction of the rapidity lines expressed in (6.2) leads to a translation invariance over π for each individual u_j separately. This only implies that λ is an even integer. Equation (6.3) gives the stronger condition $\lambda = 2$.

[6] Strictly spoken, the diagonal distance is not m, but $m\sqrt{2}$, so that the inverse diagonal correlation length really should be $|\log k|/\sqrt{2}$ agreeing with (5.21) in the limit $k \to 1$.

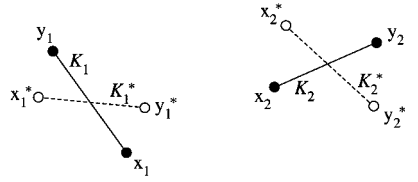

Fig. 11. Part of an Ising model and its dual on a general planar graph: Indicated are two neighbor pairs of spins indicated by small black circles with their reduced interaction constants K_i (drawn lines). Also indicated are their corresponding two pairs of dual spins indicated by white circles with their reduced interaction constants K_i^* (dashed lines). Note that both $(\mathrm{x}_1, \mathrm{x}_1^*, \mathrm{y}_1, \mathrm{y}_1^*)$ and $(\mathrm{x}_2, \mathrm{x}_2^*, \mathrm{y}_2, \mathrm{y}_2^*)$ are arranged clockwise.

see also Fig. 11. Here we have two arbitrarily chosen unequal nearest-neighbor pairs of spins at the sites $\{\mathrm{x}_1, \mathrm{y}_1\} \neq \{\mathrm{x}_2, \mathrm{y}_2\}$ with couplings $K_1 = \beta J_1$, and $K_2 = \beta J_2$. Also we have their corresponding two nearest-neighbor pairs of dual spins at sites $\{\mathrm{x}_1^*, \mathrm{y}_1^*\}$ and $\{\mathrm{x}_2^*, \mathrm{y}_2^*\}$ with couplings K_1^* and K_2^* satisfying $\sinh(2K_i)\sinh(2K_i^*) = 1$, $(i = 1, 2)$. The orientations of the two quadruples of points $(\mathrm{x}_1, \mathrm{x}_1^*, \mathrm{y}_1, \mathrm{y}_1^*)$ and $(\mathrm{x}_2, \mathrm{x}_2^*, \mathrm{y}_2, \mathrm{y}_2^*)$ must both be chosen the same for (6.9) to hold with a plus sign on the second line. Many results can be derived from this one equation alone, which is an ultimate statement of the fermionic character of the Ising model. In particular, (3.6)–(3.8) are specializations of (6.9) to the uniform symmetric square lattice.[15]

Restricting ourselves to the Z-invariant Ising model the quadratic identity reduces to

$$\begin{aligned} & k^2 \operatorname{sc}(u_2 - u_1, k') \operatorname{sc}(u_4 - u_3, k') \\ & \quad \times \{ g(u_1, u_2, u_3, u_4, \ldots)\, g(\cdots) - g(u_1, u_2, \ldots)\, g(u_3, u_4, \ldots) \} \\ & \quad + \{ g^*(u_1, u_3, \ldots)\, g^*(u_2, u_4, \ldots) - g^*(u_1, u_4, \ldots)\, g^*(u_2, u_3, \ldots) \} = 0 \end{aligned} \tag{6.10}$$

suppressing all arguments but the four rapidity variables that differ among the two-point functions g and g^*. This result is easily derived assuming that all rapidity lines pass between the spins in the same direction. Equation (6.10) is also applicable if some of the rapidity lines go in the opposite direction, providing the corresponding u_j are replaced by $u_j + \mathrm{K}(k')$, as discussed above.

In the scaling limit $k \to 1$, $k' \to 0$, (6.10) reduces to the leading term of

$$\begin{aligned} & \tan(u_2 - u_1) \tan(u_4 - u_3) \{ F(r_{1234})\, F(r) - F(r_{12})\, F(r_{34}) \} \\ & \quad + \{ G(r_{13})\, G(r_{24}) - G(r_{14})\, G(r_{23}) \} = 0 \end{aligned} \tag{6.11}$$

where we introduced the notations r for the scaled distance given in (6.6) with only the u_j variables common to all eight two-point functions occurring and $r_{ij\ldots}$ for the scaled distance with the variables u_i, u_j,... added. Also, F and G are the scaling limit functions corresponding to g and g^*, see (6.8). More specifically, we can write

$$r\cos\psi = \tfrac{1}{2}\xi^{-1} \sum_{j\neq 1,2,3,4} \cos(2u_j), \qquad r\sin\psi = \tfrac{1}{2}\xi^{-1} \sum_{j\neq 1,2,3,4} \sin(2u_j) \tag{6.12}$$

Since $\xi \to \infty$ the few omitted terms are infinitesimally small.

Expanding to second order and doing straightforward manipulations we arrive at

$$\begin{aligned}&\cos(u_1+u_2-\psi)\cos(u_3+u_4-\psi)(FF''-F'^2+r^{-1}GG')\\&\quad+\sin(u_1+u_2-\psi)\sin(u_3+u_4-\psi)(GG''-G'^2+r^{-1}FF')=0\end{aligned} \tag{6.13}$$

where the primes denote differentiation with respect to r. Since this must hold for all values of ψ, we conclude

$$FF''-F'^2 = -r^{-1}GG' \tag{6.14}$$

$$GG''-G'^2 = -r^{-1}FF' \tag{6.15}$$

These are the same equations as those that would follow from the quadratic identities for the rotational-invariant scaling functions of the uniform case.

6.3. Painlevé Equations

We can take the first derivative of (6.14), i.e.,

$$FF'''-F'F'' = -r^{-1}GG''-r^{-1}G'^2+r^{-2}GG' \tag{6.16}$$

Eliminating G' and G'' from (6.16) using (6.14) and (6.15), we find

$$G^2 = \frac{-2r^3(FF''-F'^2)^2}{r^2(FF'''-F'F'')+r(FF''-F'^2)-FF'} \tag{6.17}$$

Taking the first derivative of this and substituting it in (6.14), we find a closed equation for $F(r)$, namely

$$\begin{aligned}&(FF''-F'^2)(r^4F''''-2r^2F''+rF')+FF'^2\\&\quad+r^4(2F'F''F'''-FF'''^2-F''^3)=0\end{aligned} \tag{6.18}$$

Clearly, $G(r)$ satisfies the same equation. Following Jimbo and Miwa[36] we can change to a new dependent variable

$$\zeta = rF'/F \tag{6.19}$$

which satisfies

$$r^3(\zeta'\zeta''' - \zeta''^2) - r^2(\zeta\zeta''' - \zeta'\zeta'') - r\zeta\zeta'' + \zeta\zeta' + 2r^2\zeta'^3 - 6r\zeta\zeta'^2 + 4\zeta^2\zeta' = 0 \tag{6.20}$$

This can be integrated once as

$$\frac{r^2\zeta''^2 + 4\zeta'^2(r\zeta' - \zeta) - \zeta'^2}{4(r\zeta' - \zeta)^2} = \mu^2 \tag{6.21}$$

where μ is a constant setting the scale. Hence, we arrive at the Painlevé V equation[36, 38]

$$(r\zeta'')^2 = 4\mu^2(r\zeta' - \zeta)^2 - 4\zeta'^2(r\zeta' - \zeta) + \zeta'^2 \tag{6.22}$$

and its derivative

$$r^2\zeta''' + r\zeta'' = 4\mu^2 r(r\zeta' - \zeta) - 4\zeta'(r\zeta' - \zeta) + 2r\zeta'^2 + \zeta' \tag{6.23}$$

Equations (6.18) and (6.20) are recovered again by eliminating μ^2 between the last two equations. Comparing with the result for the uniform rectangular case,[11, 38] we see that we must set $\mu = 1$. Originally these scaling functions $F(r)$ and $G(r)$ were given in terms of a Painlevé III formulation,[11] but this has been shown to agree with the Painlevé V version.[38]

We conclude this section noting that we have found the scaled correlation only for regimes I and II ($k < 1$ or $k > 1$). There is a third regime III with k purely imaginary.[12, 13] For this case, we expect the scaled correlation function to be given in terms of products of two Painlevé V functions, as the correlation functions factorize.[37]

7. FERROMAGNETIC *Z*-INVARIANT FIBONACCI ISING MODEL

In Section 5 we have studied Fibonacci Ising Models with interactions that are attractive or repulsive according to Fibonacci rules. We shall now consider Fibonacci Ising Models with purely ferromagnetic interactions.

If the Ising couplings are all ferromagnetic, then the connected two-point correlation function remains strictly positive for all distances because

of the second Griffiths inequality.[54–56] Therefore, the oscillations—if any—are much smaller than in the mixed-sign case.

If the variation in the Ising couplings is small, the correlation function is expected to decay monotonically. This can be seen as follows: In such a ferromagnetic Fibonacci Ising model the pair interactions may take several values and we denote the smallest one by K_s and the largest one by K_g. For fixed distance, we can then use the Griffiths inequalities to show that the correlation function of this ferromagnetic Fibonacci Ising lattice is larger than that of the uniform ferromagnetic Ising lattice whose pair interaction is equal K_s, and smaller than that of the uniform lattice with K_g. Since the correlation functions of these two uniform ferromagnetic Ising models are monotonically decreasing functions of distance, it is therefore unlikely that the aperiodic lattice would behave much different from the regular Ising lattice.

Indeed, in none of our numerical calculations on the Z-invariant Fibonacci Ising Model did we encounter clearly visible multiple peaks in $\chi(\mathbf{q})$ as in Section 5. Instead, we only observed a single clear peak at $\mathbf{q}=0$, even though those computations were more involved, using the more general quadratic relations (6.9) together with the determinant calculations of diagonal and next-to-diagonal correlation functions mentioned in Subsection 4.1.

Rather than going through those calculations in further detail, we shall first summarize our results for the one-dimensional case and then argue that in the scaling limit, using the results of Section 6, $\chi(\mathbf{q})$ has a universal form for all ferromagnetic Z-invariant Fibonacci Ising Models.

7.1. One-Dimensional Example

It is by now well-known that for the general Ising chain in zero field with interaction energy

$$\mathscr{E}/k_{\mathrm{B}}T = -\sum_{n} K_n \sigma_n \sigma_{n+1} \tag{7.1}$$

the pair correlation function is simply given by

$$\langle \sigma_m \sigma_n \rangle = \prod_{l=\min(m,\,n)}^{\max(m,\,n)-1} \tanh K_l, \qquad |\tanh K_l| \equiv \exp(-1/\xi_l) \tag{7.2}$$

with ξ_l the correlation length for the uniform case with all couplings equal K_l. Therefore, it takes only little effort to plot $\chi(q)$ for the case that the $\{K_j\}$ form a Fibonacci sequence of K_{A} and K_{B}, with the K_{A} more abundant.

As in Section 5, we can find the effective pair correlation using Tracy's Lemma 2.5.[39] In the case that $K_{\mathbf{A}}$ and $K_{\mathbf{B}}$ are both ferromagnetic, we find

$$k_{\mathbf{B}}T\chi(q) = 1 + 2\sum_{n=1}^{\infty} C^{(\mathrm{c})}(n)\cos(qn) \tag{7.3}$$

with

$$\begin{aligned} C^{(\mathrm{c})}(n) = C^{(\mathrm{c})}(-n) &= (1-\{\alpha n\})\,\mathrm{e}^{-\lfloor \alpha n\rfloor/\xi_{\mathbf{A}}}\mathrm{e}^{-(n-\lfloor \alpha n\rfloor)/\xi_{\mathbf{B}}} \\ &\quad + \{\alpha n\}\,\mathrm{e}^{-(\lfloor \alpha n\rfloor+1)/\xi_{\mathbf{A}}}\mathrm{e}^{-(n-\lfloor \alpha n\rfloor-1)/\xi_{\mathbf{B}}}, \qquad (n\geqslant 0) \end{aligned} \tag{7.4}$$

Using the theory of Fourier series, we can then rewrite (7.4) as

$$\begin{aligned} C^{(\mathrm{c})}(n) &= (1+(\mathrm{e}^{\delta}-1)\{\alpha n\})\,\mathrm{e}^{-\delta\{\alpha n\}}\mathrm{e}^{-\kappa n} \\ &= \sum_{m=-\infty}^{\infty} \frac{\sinh^2\frac{1}{2}\delta}{(\frac{1}{2}\delta+\pi\mathrm{i}m)^2}\,\mathrm{e}^{2\pi\mathrm{i}m\alpha n-\kappa n}, \qquad (n\geqslant 0) \end{aligned} \tag{7.5}$$

where

$$\delta = \frac{1}{\xi_{\mathbf{B}}} - \frac{1}{\xi_{\mathbf{A}}}, \qquad \kappa = \frac{\alpha}{\xi_{\mathbf{A}}} + \frac{1-\alpha}{\xi_{\mathbf{B}}} \tag{7.6}$$

When $K_{\mathbf{A}} < 0$, we still have (7.3), but we have to replace $1/\xi_{\mathbf{A}}$ by $1/\xi_{\mathbf{A}} - \pi\mathrm{i}$ in (7.4) and (7.6), or δ has to be replaced by $\delta+\pi\mathrm{i}$ and κ by $\kappa-\pi\mathrm{i}\alpha$.

Since the effective correlation function (7.4) decays exponentially, it is trivial to calculate the sum (7.3) numerically using software packages like Maple. Therefore, without too many further details we shall present plots for four cases in Fig. 12.

The first plot is for the uniform ferromagnetic case at three different temperatures, with the highest and sharpest peak at $q=0$ for the lowest temperature. The reduced wavevector-dependent susceptibility in this case is given by

$$k_{\mathbf{B}}T\chi_0(q) = \frac{\sinh\xi^{-1}}{\cosh\xi^{-1}-\cos q}, \qquad \xi^{-1} = -\log\tanh K \tag{7.7}$$

The peaks get higher and narrower as the temperature goes down, while the area under the curve remains constant, namely 2π.

The second plot is for the case that $\xi_{\mathbf{A}}$ and $\xi_{\mathbf{B}}$ have a ratio of 4:1. It is hard to see any difference with the first plot; this is also true for the case

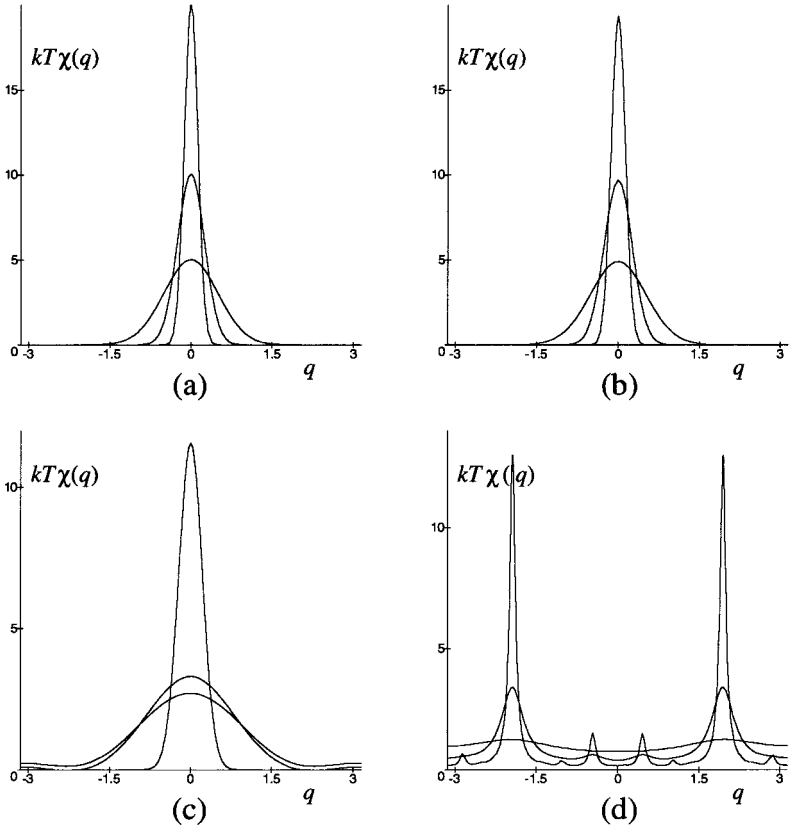

Fig. 12. Reduced wavevector dependent susceptibility $k_B T\chi(q)$ for the one-dimensional Ising chain. The four cases are: (a) the uniform ferromagnetic case; (b) the 4:1 Fibonacci case; (c) the 2^{26}:1 Fibonacci case; and (d) the mixed-sign 1:1 Fibonacci case. See text.

with ratio 1:4, which is not shown. The third case has ratio 2^{26}:1, very close to the decoupling limit; even though there is a clear quantitative difference, qualitatively it still looks like the uniform case. Indeed, in the ferromagnetic Fibonacci case we have from (7.3) and (7.5) that

$$k_B T\chi(q) = \sum_{m=-\infty}^{\infty} \frac{\sinh^2 \frac{1}{2}\delta}{(\frac{1}{2}\delta + \pi i m)^2} \frac{\sinh(\kappa - 2\pi i m\alpha)}{\cosh(\kappa - 2\pi i m\alpha) - \cos q} \tag{7.8}$$

In the limit $T \to T_c = 0$, both δ and κ tend to zero exponentially fast, and it is not difficult to see that the $m = 0$ term totally dominates (7.8), or $\chi(q) \approx \chi_0(q)$ with $\xi^{-1} = \kappa$. This clear universal behavior, with only a single delta-function divergence at $q = 0$, holds as long as both K_A and K_B are

positive. Similarly, when K_A and K_B are both negative there is only one divergence at $q=\pi$, as $\chi(q)$ then equals $\chi(q\pm\pi)$ of the ferromagnetic case.

The final plot is for the mixed case with ferro- and antiferromagnetic couplings of equal strength, which is the one-dimensional version of the cases in Section 5. This last case is very different with clear incommensurate peaks at the lowest temperature. In this mixed case, using the theory of Section 5 or alternatively using (7.8) with $\delta=\pi\mathrm{i}$, we have

$$\chi_{\mathrm{m}}(q)=\sum_{m=-\infty}^{\infty}\frac{1}{(m+\frac{1}{2})^2\pi^2}\,\chi_0(q+2\pi(m+\tfrac{1}{2})\,\alpha),\qquad \alpha=\tfrac{1}{2}(\sqrt{5}-1) \tag{7.9}$$

indicating the locations and heights of the visible peaks. In fact, $\chi_0(q)$ is periodic mod 2π, so that the peaks are located at $q=2\pi(m+\frac{1}{2})\,\alpha+2\pi n$, with m and n arbitrary integers. The number of visible peaks increases as the temperature decreases and the correlation length ξ increases. It does not matter that we have chosen the antiferromagnetic coupling to be the more abundant one, as the other case follows from this one simply replacing $\chi(q)\to\chi(q\pm\pi)$, corresponding to a flip of sign of every other spin.

It may be worthwhile to note that also in this mixed case we have strong universality, with $\chi(q)\approx\chi_{\mathrm{m}}(q)$ as $T\to 0$. Now $\delta\to\pi\mathrm{i}$ instead of 0, causing all terms in (7.8) to contribute, rather than just the $m=0$ term.

7.2. Two-Dimensional Fibonacci Ising Model in the Scaling Limit

We shall now study the simplest two-dimensional ferromagnetic case, which is the Z-invariant Ising model with quasiperiodicity in one or two diagonal directions.

This model is described in terms of two perpendicular sets of diagonal rapidity lines, shown in Fig. 9. The rapidity variables $\{u_j\}$ and $\{v_j\}$ form the Fibonacci sequences $\{u_A, u_B, u_A, u_A, u_B,\ldots\}$ and $\{v_A, v_B, v_A, v_A, v_B,\ldots\}$. If $v_A=v_B$, the aperiodicity in the corresponding diagonal direction disappears. As shown in Fig. 9, the rapidity lines define a checkerboard lattice with alternatingly black and white faces, where the order variables (spins $\sigma=\pm 1$) and disorder variables (dual spins $\mu\equiv\sigma^*$) live. Two adjacent spins share one vertex which is the intersection of two rapidity lines u_i and v_j.

The pair interaction energies between such pairs of spins are either K_{ij} shown in Fig. 10a, or $\bar{K}_{ij}$ shown in Fig. 10b. We have given a real elliptic parametrization in (6.1). Two other parametrizations have been used by Baxter[12, 13] and Martínez.[18, 19] They are

$$\sinh 2K_{ij}=-ik\,\mathrm{sn}(\mathrm{i}u_i-\mathrm{i}v_j,k),\qquad \sinh 2\bar{K}_{ij}=\mathrm{i}/\mathrm{sn}(\mathrm{i}u_i-\mathrm{i}v_j,k) \tag{7.10}$$

suitable for $T > T_c$ (or $k < 1$) and

$$\sinh 2K_{ij} = -\mathrm{i}\,\mathrm{sn}(\mathrm{i}u'_i - \mathrm{i}v'_j, 1/k), \qquad \sinh 2\bar{K}_{ij} = \mathrm{i}k/\mathrm{sn}(\mathrm{i}u'_i - \mathrm{i}v'_j, 1/k) \tag{7.11}$$

more suited for $T < T_c$ (or $k > 1$). This last representation involves an implicit rescaling of the rapidity variables by a factor k, $u'_i = ku_i$, $v'_j = kv_j$, in view of Jacobi's real transformation $k\,\mathrm{sn}(x, k) = \mathrm{sn}(kx, 1/k)$.

The pair correlation functions of the order and disorder variables have been discussed in Section 6. Therefore, we can write

$$\begin{aligned} \langle \sigma_{m,n}\sigma_{m',n'} \rangle &= g_{2m'-2m}(k; u_{m-n+1},..., u_{m'-n'}, v_{m+n},..., v_{m'+n'-1}), \\ \langle \sigma^*_{m,n}\sigma^*_{m',n'} \rangle &= g^*_{2m'-2m}(k; u_{m-n+1},..., u_{m'-n'}, v_{m+n+1},..., v_{m'+n'}) \end{aligned} \tag{7.12}$$

assuming $m+n \leqslant m'+n'$ and $m-n \leqslant m'-n'$, in which case all rapidity lines pass between the spins (or dual spins) in the same direction. Clearly, the same result holds if $m+n \geqslant m'+n'$ and $m-n \geqslant m'-n'$, interchanging (m, n) with (m', n'). On the other hand, if $m+n \leqslant m'+n'$ and $m-n \geqslant m'-n'$, we have

$$\begin{aligned} \langle \sigma_{m,n}\sigma_{m',n'} \rangle &= g_{2n'-2n}(k; u_{m'-n'+1},..., u_{m-n}, \bar{v}_{m+n},..., \bar{v}_{m'+n'-1}), \\ \langle \sigma^*_{m,n}\sigma^*_{m',n'} \rangle &= g^*_{2n'-2n}(k; u_{m'-n'+1},..., u_{m-n}, \bar{v}_{m+n+1},..., \bar{v}_{m'+n'}) \end{aligned} \tag{7.13}$$

where $\bar{v}_j = v_j + \mathrm{K}(k')$. Finally, for $m+n \geqslant m'+n'$ and $m-n \leqslant m'-n'$, we have to interchange (m, n) with (m', n') in (7.13). There exist several multiple integral, determinant, and Pfaffian representations[12, 16–19] for these functions g_{2m}. In our study of the Fibonacci Ising model, it is not necessary to use any of these results. We can use quadratic recurrence relations instead as is explained in Section 6.

7.3. Effective Connected Pair Correlation Function in the Scaling Limit

If we assume that the rapidity variables take at most four different values $u_1,..., u_4$ and if we let M_j be the number of times that the value u_j occurs as argument of a given g_{2m} function, then we can define the shorthand notation

$$G(M_1, M_2, M_3, M_4) = g^{(c)}_{2m}(k; \overbrace{u_1,..., u_1}^{M_1}, \overbrace{u_2,..., u_2}^{M_2}, \overbrace{u_3,..., u_3}^{M_3}, \overbrace{u_4,..., u_4}^{M_4}) \tag{7.14}$$

with $M_1 + M_2 + M_3 + M_4 = 2m$. Next, if we write $u_1 = u_{\mathrm{A}}$, $u_2 = u_{\mathrm{B}}$, $u_3 = v_{\mathrm{A}}$, $u_4 = v_{\mathrm{B}}$ for the Fibonacci Ising model of this section, then we can apply

Lemma 2.5 in ref. 39 as we did in Section 5. This yields the effective connected pair correlation function

$$\begin{aligned} C^{(c)}(m,n) &= \lim_{\mathscr{L}\to\infty} \mathscr{L}^{-2} \sum_{m',n'} \langle \sigma_{m',n'}\sigma_{m'+m,n'+n}\rangle^{(c)} \\ &= (1-\{(m+n)\,\alpha\})(1-\{(m-n)\,\alpha\})\, G(N_1, N_2, N_3, N_4) \\ &\quad + (1-\{(m+n)\,\alpha\})\{(m-n)\,\alpha\}\; G(N_1+1, N_2-1, N_3, N_4)) \\ &\quad + \{(m+n)\,\alpha\}(1-\{(m-n)\,\alpha\})\, G(N_1, N_2, N_3+1, N_4-1) \\ &\quad + \{(m+n)\,\alpha\}\{(m-n)\,\alpha\}\; G(N_1+1, N_2-1, N_3+1, N_4-1) \end{aligned} \tag{7.15}$$

where

$$\begin{aligned} N_1 &= m-n-N_2 = \lfloor (m-n)\,\alpha \rfloor, \\ N_3 &= m+n-N_4 = \lfloor (m+n)\,\alpha \rfloor \end{aligned} \tag{7.16}$$

The Fourier transform of (7.15) gives the exact q-dependent susceptibility.

We have already seen that at temperatures for which the correlation length is short, the q-dependent susceptibility of the aperiodic lattice does not show much difference from that of the periodic lattice. We really need only to examine the case that T is close to T_c. For the remainder of this section we shall restrict ourselves to the scaling limit and use the results of Section 6. From (6.7) and (6.8) we find

$$g^{(c)}_{2m}(k; u_1, \ldots, u_{2m}) \approx |1-k^{-2}|^{1/4}\, f_{\pm}(|t|\, R) \tag{7.17}$$

with $t = 1-k$ and with f_+ and f_- the connected versions of F and G. In other words, f_- for $T < T_c$ includes a subtraction of the contribution due to the square of the spontaneous magnetization. For correlation functions of the form (7.14), (6.6) reduces to

$$\begin{aligned} 4R^2 &= (M_1 \cos 2u_1 + M_2 \cos 2u_2 + M_3 \cos 2u_3 + M_4 \cos 2u_4)^2 \\ &\quad + (M_1 \sin 2u_1 + M_2 \sin 2u_2 + M_3 \sin 2u_3 + M_4 \sin 2u_4)^2 \end{aligned} \tag{7.18}$$

If the rapidity lines with rapidity variable u_j pass between the two spins in the opposite direction compared to a preferred direction, we have to replace u_j by $u_j \pm \mathrm{K}(0) = u_j \pm \frac{1}{2}\pi$, as explained in Section 6.1. Equivalently, we can replace $M_j > 0$ by $-M_j < 0$. Because of this, R continues smoothly across a boundary where $M_j = 0$.

The spin correlation function of the regular two-dimensional Ising model has this scaling form with $u_1 = u$ and $u_2 = v$, whereas u_3 and u_4 are absent. More precisely, (7.17) reduces to

$$\langle \sigma_{0,0}\sigma_{m,n}\rangle^{(c)} = G(m-n, m+n, 0, 0) \approx |1-k^{-2}|^{1/4} f_{\pm}(|t|\, R) \tag{7.19}$$

with

$$R = \sqrt{m^2 \cos^2(u-v) + n^2 \sin^2(u-v)} \tag{7.20}$$

Here one may have assumed that $m+n,\ m-n \geqslant 0$. However, (7.20) is valid generally for R large taking in account the remark below (7.18). Therefore, the scaled correlation function is indeed rotationally invariant and, as shown also in Section 6.3, it is given in terms of Painlevé equations.[11, 36, 38]

In order to compare with Vaidya's[35] work on the triangular Ising model, we must study a quadratic Ising model with "SW-NE" diagonal interactions. At criticality, the horizontal interactions K_1, the vertical interactions K_2, and the diagonal interactions K_3 are given by

$$\sinh 2K_1 = \tan(u_1 - u_3), \qquad \sinh 2K_2 = \tan(u_3 - u_2),$$
$$\sinh 2K_3 = \cot(u_1 - u_2) \tag{7.21}$$

Here we have vertical rapidities u_1 pointing north, horizontal rapidities u_2 pointing east, and diagonal rapidities u_3 pointing northeast. Each rapidity line intersects each bonds it meets in the middle. Using (7.18), we find that the scaled correlation function is given by

$$\langle \sigma_{0,0}\sigma_{m,n}\rangle^{(c)} = G(m, -n, m-n, 0), \qquad \text{for} \quad m \geqslant 0 \quad \text{and} \quad n \leqslant 0 \tag{7.22}$$

Substituting M_i and u_i into (7.18), rewriting $u_1 = u$, $u_2 = v$, $u_3 = w$, we find that vector (m, n) corresponds to the scaled distance

$$R^2 = m^2 \cos(u-w)^2 + n^2 \cos(v-w)^2$$
$$- 2mn \cos(u-w) \cos(v-w) \cos(u-v) \tag{7.23}$$

Again, taking in account the remark below (7.18), (7.23) gives R also for the regions with $m < 0$ or $n > 0$. This result for R is proportional to the one of Vaidya[35] after some simplifications and after identifying $N \equiv m$, $M \equiv n$. Equation (7.23) gives the most general positive definite quadratic form in m and n. Therefore, the scaled correlation function of the most general periodic Z-invariant Ising model cannot be distinguished from that of the triangular lattice.

7.4. Wavevector-Dependent Susceptibility of the Fibonacci Ising Model in the Scaling Limit

The effective pair correlation of the Z-invariant Fibonacci Ising model has been evaluated exactly in (7.15). We now use (7.17) with R given by (7.18) to rewrite it in the scaling limit as

$$\begin{aligned} C^{(c)}(m,n)\,|1-k^{-2}|^{-1/4} \\ \approx f_{\pm}(|t|\,R_1)+\{(m-n)\,\alpha\}[f_{\pm}(|t|\,R_2)-f_{\pm}(|t|\,R_1)] \\ +\{(m+n)\,\alpha\})[f_{\pm}(|t|\,R_3)-f_{\pm}(|t|\,R_1)] \\ +\{(m-n)\,\alpha\}\{(m+n)\,\alpha\}[f_{\pm}(|t|\,R_1)-f_{\pm}(|t|\,R_2)-f_{\pm}(|t|\,R_3) \\ +f_{\pm}(|t|\,R_4)] \end{aligned} \tag{7.24}$$

where $u_1=u_{\mathrm{A}}$, $u_2=u_{\mathrm{B}}$, $u_3=v_{\mathrm{A}}$, and $u_4=v_{\mathrm{B}}$. The R_j, for $j=1, 2, 3, 4$, follow from (7.18) with the substitutions

$$\begin{aligned} R_1&: (M_1, M_2, M_3, M_4)=(N_1, N_2, N_3, N_4) \\ R_2&: (M_1, M_2, M_3, M_4)=(N_1+1, N_2-1, N_3, N_4) \\ R_3&: (M_1, M_2, M_3, M_4)=(N_1, N_2, N_3+1, N_4-1) \\ R_4&: (M_1, M_2, M_3, M_4)=(N_1+1, N_2-1, N_3+1, N_4-1) \end{aligned} \tag{7.25}$$

in accordance with (7.15). Since $\lfloor \alpha(m\pm n)\rfloor \approx \alpha(m\pm n)$ for m, n large, we expand the R_j around R_0, which is given by

$$\begin{aligned} 4R_0^2=&[(m-n)(\alpha\cos 2u_{\mathrm{A}}+(1-\alpha)\cos 2u_{\mathrm{B}}) \\ &+(m+n)(\alpha\cos 2v_{\mathrm{A}}+(1-\alpha)\cos 2v_{\mathrm{B}})]^2 \\ &+[(m-n)(\alpha\sin 2u_{\mathrm{A}}+(1-\alpha)\sin 2u_{\mathrm{B}}) \\ &+(m+n)(\alpha\sin 2v_{\mathrm{A}}+(1-\alpha)\sin 2v_{\mathrm{B}})]^2 \end{aligned} \tag{7.26}$$

which has the general quadratic form $A(m-an)^2+B(n+am)^2$ with A, B, and a some constants, no more general than Vaidya's form[35] for the triangular lattice (7.23).

It is straightforward to verify that

$$\begin{aligned} R_1-R_0+\{(m-n)\,\alpha\}(R_2-R_1)+\{(m+n)\,\alpha\}(R_3-R_1)=\mathrm{O}(R_0^{-1}), \\ R_i-R_0=\mathrm{O}(1), \qquad R_1-R_2-R_3+R_4=\mathrm{O}(R_0^{-1}) \end{aligned} \tag{7.27}$$

when $R_0 \to \infty$. Also, we can Taylor expand

$$f_{\pm}(|t|\ R_i) = f_{\pm}(|t|\ R_0) + |t|\ (R_i - R_0)\ f'_{\pm}(|t|\ R_0) + \cdots \tag{7.28}$$

Therefore, in the scaling limit, we find that (7.24) becomes

$$C^{(c)}(m, n) \approx |1 - k^{-2}|^{1/4}\ f_{\pm}(|t|\ R_0) \tag{7.29}$$

where the error is of the same order of magnitude as corrections to scaling. In the scaling limit, we have to ignore those higher-order corrections and substitute (7.29) into (5.6), converting the sum to an integral. It is easily seen by comparing (7.29) with (7.20) that the only difference is the change in R, which corresponds to a combination of a rotation and a scale transformation. Hence, the scaled q-dependent susceptibility of the Z-invariant ferromagnetic Fibonacci Ising model is the same as the one of a ferromagnetic Ising model on a triangular lattice. There is only one peak at $q_x = q_y = 0 \bmod 2\pi$, whose height is given by (5.15), except for a change in the constant $c_{\pm}$. This is another manifestation of universality.

8. CONCLUSIONS

Even though several authors have shown that the quasi-periodic Ising model is in the same universality class as the regular Ising model, with the same critical exponents, its wavevector-dependent susceptibility can have multiple incommensurate peaks. However, this only happens when the pair interactions are both attractive and repulsive and the sign of the interactions varies in an incommensurate way.

Indeed, for the mixed Fibonacci Ising model (with an incommensurate sequence of ferro- and antiferromagnetic bonds), $\chi(\mathbf{q})$ has infinitely many divergencies at T_c, which are everywhere dense in the unit cell $0 \leqslant q_x, q_y \leqslant 2\pi$. Away from T_c there is a finite number of incommensurate peaks, and more and more of these peaks become invisible as T moves farther away from T_c.

When all pair interactions are ferromagnetic, however, the q-dependent susceptibility behaves just like the one in the regular ferromagnetic Ising model, with only one diverging peak per unit cell located at $(q_x, q_y) = (0, 0)$, in spite of aperiodicity present in the lattice. This is explained by the fact that the spin correlation function in a ferromagnetic Ising Fibonacci lattice decays as a function of distance without changing sign. We have shown this in two examples, the one-dimensional case ($T_c = 0$) in Section 7.1 and the scaling limit of the Z-invariant Ising model in Section 7.4.

In other words, when there are no oscillations in the pair correlation, then there is no trace of the multi-peaks in the q-dependent susceptibility. This is a confirmation of work by Nelson and Widom, that the interference pattern in the icosahedral alloy is a result of the many oscillations in the radial pair correlation functions.[57–59]

Not only does the wavevector-dependent susceptibility $\chi(\mathbf{q})$ have but one pronounced peak at $\mathbf{q}=(0, 0)$, leading to a single $T=0$ divergence, if all the interactions are ferromagnetic; also if the interactions on the quadratic lattice are purely antiferromagnetic we expect only one such peak at $\mathbf{q}=(\pi, \pi)$, even if the magnitudes of the interactions vary quasiperiodically.

For the other cases that we considered, with aperiodic mixed signs of the bonds, the pair correlations as seen from (5.8), (5.22)–(5.26) pick up oscillating phase factors. These factors are present for both $T>T_c$ and $T<T_c$. Thus it follows that the everywhere dense set of overlapping peaks is a result of aperiodic oscillations of the pair correlations; whether the system is ordered or disordered is not relevant. The difference in the number of peaks at different temperatures shows that the number of oscillations per correlation length in the pair correlation function determines the number of visible peaks.

If—instead of aperiodic oscillations—the pair correlation picks up a periodic phase factor, then the diffraction patterns as well as the q-dependent susceptibilities in the two cases differ in two ways. As the correlation length increases, the peaks move and approach their different sets of positions for the two cases, one commensurate and the other incommensurate. Moreover, as $\xi \to \infty$ there is an ever-increasing number of peaks for the aperiodic case, while the number of peaks for the periodic case has an upper bound.

Finally, in our present paper we have chosen the underlying lattice to be regular. With our increased knowledge of the correlation functions we should be able to repeat the calculations for certain aperiodic lattices[22–29, 60, 61] like Penrose tilings. We hope to come back to this in a future publication.

ACKNOWLEDGMENTS

We thank Dr. R. J. Baxter for many years of helpful and stimulating comments. We are grateful to the organizing committee for providing us with an opportunity to visit Canberra again and to have many fruitful discussions during the conference. We also thank Dr. J. de Gier, Dr. U. Grimm, Dr. C. L. Henley, Dr. B. Nienhuis, Dr. A. Sokal, Dr. C. A. Tracy, and Dr. M. Widom for helpful discussions and correspondence on quasicrystals. Supported in part by NSF Grants PHY 97-22159 and PHY 97-24788.

REFERENCES

1. R. J. Baxter, *Exactly Solved Models in Statistical Mechanics* (Academic, London, 1982).
2. L. Onsager, Crystal statistics. I. A two-dimensional model with an order-disorder transition, *Phys. Rev.* **65**:117–149 (1944).
3. B. Kaufman, Crystal statistics. II. Partition function evaluated by spinor analysis, *Phys. Rev.* **76**:1232–1243 (1949).
4. B. Kaufman and L. Onsager, Crystal statistics. III. Short-range order in a binary Ising lattice, *Phys. Rev.* **76**:1244–1252 (1949).
5. L. Onsager, Discussion, *Nuovo Cimento (Ser. 9)* **6**(Suppl.):261 (1949).
6. C. N. Yang, The spontaneous magnetization of a two-dimensional Ising model, *Phys. Rev.* **85**:808–816 (1952).
7. E. W. Montroll, R. B. Potts, and J. C. Ward, Correlations and spontaneous magnetization of the two-dimensional Ising model, *J. Math. Phys.* **4**:308–322 (1963).
8. T. T. Wu, Theory of Toeplitz determinants and the spin correlations of the two-dimensional Ising model. I, *Phys. Rev.* **149**:380–401 (1966).
9. L. P. Kadanoff, Spin-spin correlations in the two-dimensional Ising model, *Nuovo Cimento (Ser. 10) B* **44**:276–305 (1966).
10. B. M. McCoy and T. T. Wu, *The Two-Dimensional Ising Model* (Harvard University Press, Cambridge, Mass, 1973).
11. T. T. Wu, B. M. McCoy, C. A. Tracy, and E. Barouch, Spin-spin correlation functions for the two-dimensional Ising model: Exact theory in the scaling region, *Phys. Rev. B* **13**: 316–374 (1976).
12. R. J. Baxter, Solvable eight vertex model on an arbitrary planar lattice, *Phil. Trans. R. Soc. Lond. A* **289**:315–346 (1978).
13. R. J. Baxter, Free-fermion, checkerboard and Z-invariant lattice models in statistical mechanics, *Proc. R. Soc. Lond. A* **404**:1–33 (1986).
14. H. Au-Yang and J. H. H. Perk, Toda lattice equation and Wronskians in the 2D Ising model, *Physica D* **18**:365–366 (1986).
15. J. H. H. Perk, Quadratic identities for Ising correlations, *Phys. Lett. A* **79**:3–5 (1980).
16. H. Au-Yang and J. H. H. Perk, Critical correlations in a Z-invariant inhomogeneous Ising model, *Physica A* **144**:44–104 (1987).
17. H. Au-Yang and J. H. H. Perk, Solution of Hirota's discrete-time Toda lattice equation and the critical correlations in the Z-invariant Ising model, in *Proc. 1987 Summer Research Institute on Theta Functions*, Proc. Symp. Pure Math., Vol. 49, Part 1, L. Ehrenpreis and R. C. Gunning, eds. (Am. Math. Soc., Providence, R.I., 1989), pp. 287–293.
18. J. R. Reyes Martínez, Correlation functions for the Z-invariant Ising model, *Phys. Lett. A* **227**:203–208 (1997).
19. J. R. Reyes Martínez, Multi-spin correlation functions for the Z-invariant Ising model, *Physica A* **256**:463–484 (1998).
20. B. Davies, O. Foda, M. Jimbo, T, Miwa, and A. Nakayashiki, Diagonalization of the XXZ Hamiltonian by vertex operators, *Commun. Math. Phys.* **151**:89–153 (1993).
21. M. Jimbo and T. Miwa, *Algebraic Analysis of Solvable Lattice Models*, Regional Conference Series in Mathematics, Nr. 85 (Am. Math. Soc., Providence, R.I., 1995).
22. N. V. Antonov and V. E. Korepin, Critical properties and correlation functions of the eight-vertex model on a quasicrystal, *Zap. Nauch. Semin. LOMI* **161**:13–23 (1987) [*J. Sov. Math.* **46**:2058–2065 (1989)].
23. N. V. Antonov and V. E. Korepin, Critical properties of completely integrable spin models in quasicrystals, *Teor. Mat. Fiz.* **77**:402–411 (1988) [*Theor. Math. Phys.* **77**:1282–1288 (1988)].

24. V. E. Korepin, Eight-vertex model of the quasicrystal, *Phys. Lett. A* **118**:285–287 (1986).
25. V. E. Korepin, Completely integrable models in quasicrystals, *Commun. Math. Phys.* **110**:157–171 (1987).
26. T. C. Choy, Ising models on two-dimensional quasi-crystals: Some exact results, *Intern. J. Mod. Phys. B* **2**:49–63 (1988).
27. M. Baake, U. Grimm, and R. J. Baxter, A critical Ising model on the labyrinth, *Intern. J. Mod. Phys. B* **8**:3579–3600 (1994).
28. U. Grimm, M. Baake, and H. Simon, Ising spins on the labyrinth, in *Proc. of the 5th International Conference on Quasicrystals*, C. Janot and R. Mosseri, eds. (World Scientific, Singapore, 1995), pp. 80–83.
29. U. Grimm and M. Baake, Aperiodic Ising models, in *The Mathematics of Long-Range Aperiodic Order*, R. V. Moody, ed. (Kluwer, Dordrecht, 1997), pp. 199–237.
30. J. A. Ashraff and R. B. Stinchcombe, Dynamic structure factor for Fibonacci-chain quasicrystal, *Phys. Rev. B* **39**:2670–2677 (1989).
31. C. A. Tracy and B. M. McCoy, Neutron scattering and the correlation functions of the two-dimensional Ising model near T_c, *Phys. Rev. Lett.* **31**:1500–1504 (1973).
32. J. Stephenson, Ising-model spin correlations on the triangular lattice, *J. Math. Phys.* **5**:1009–1024 (1964).
33. J. Stephenson, Ising-model spin correlations on the triangular lattice. II. Fourth-order correlations, *J. Math. Phys.* **7**:1123–1132 (1966).
34. J. Stephenson, Ising-model spin correlations on the triangular lattice. III. Isotropic antiferromagnetic lattice, *J. Math. Phys.* **11**:413–419 (1970).
35. H. G. Vaidya, The spin-spin correlation functions and susceptibility amplitudes for the two-dimensional Ising model: Triangular lattice, *Phys. Lett. A* **57**:1–4 (1976).
36. M. Jimbo and T. Miwa, Studies on holonomic quantum fields. XVII, *Proc. Japan Acad. A* **56**:405–410 (1980), *Errata* **57**:347 (1981).
37. H. Au-Yang and J. H. H. Perk, Ising correlations at the critical temperature, *Phys. Lett. A* **104**:131–134 (1984).
38. B. M. McCoy and J. H. H. Perk, Relation of conformal field theory and deformation theory for the Ising model, *Nucl. Phys. B* **285[FS19]**:279–294 (1987).
39. C. A. Tracy, Universality class of a Fibonacci Ising model, *J. Stat. Phys.* **51**:481–490 (1988).
40. C. A. Tracy, Universality classes of some aperiodic Ising models, *J. Phys. A* **11**:L603–L605 (1988).
41. T. C. Lubensky, Symmetry, elasticity, and hydrodynamics in quasiperiodic structures, in *Introduction to Quasicrystals*, Aperiodicity and Order, Vol. 1, M. V. Jarić, ed. (Academic Press, Boston, 1988), pp. 199–280.
42. C. L. Henley, Quasicrystal order, its origins and its consequences: A survey of current models, *Comments Cond. Mat. Phys.* **13**:59–117 (1987).
43. C. Janot, *Quasicrystals: A Primer*, 2nd ed. (Clarendon Press, Oxford, 1994).
44. D. Shechtman, I. Blech, D. R. Gratias, and J. W. Cahn, Metallic phase with long-range orientational order and no translational symmetry, *Phys. Rev. Lett.* **53**:1951–1953 (1984).
45. P. Bak and A. I. Goldman, Quasicrystallography, in *Introduction to Quasicrystals*, Aperiodicity and Order, Vol. 1, M. V. Jarić, ed. (Academic Press, Boston, 1988), pp. 143–170.
46. L. Pauling, Icosahedral and decagonal quasicrystals as multiple twins in cubic crystals, in *Extended Icosahedral Structures*, Aperiodicity and Order, Vol. 3, M. V. Jarić and D. Gratias, eds. (Academic Press, Boston, 1989), pp. 137–162.
47. P. W. Stephens, The icosahedral glass model, in *Extended Icosahedral Structures*, Aperiodicity and Order, Vol. 3, M. V. Jarić and D. Gratias, eds. (Academic Press, Boston, 1989), pp. 37–104.

48. H. Simon and M. Baake, Lee–Yang zeros in the scaling region of a two-dimensional quasiperiodic Ising model, *J. Phys. A* **30**:5319–5327 (1997).
49. S. M. Bhattacharjee, J.-S. Ho, and J. A. Y. Johnson, Translational invariance in critical phenomena: Ising model on a quasi-lattice, *J. Phys. A* **20**:4439–4448 (1987).
50. J. P. Lu, T. Odagaki, and J. L. Birman, Properties of one-dimensional quasilattices, *Phys. Rev. B* **33**:4809–4817 (1986).
51. H. Au-Yang and B. M. McCoy, Theory of layered Ising models: Thermodynamics, *Phys. Rev. B* **10**:886–891 (1974).
52. J. R. Hamm, Regularly spaced blocks of impurities in the Ising model: Critical temperature and specific heat, *Phys. Rev. B* **15**:5391–5411 (1977).
53. B. Nickel, Private Communication. The method is also used in: W. P. Orrick, B. Nickel, A. J. Guttmann, and J. H. H. Perk, *The Susceptibility of the Square Lattice Ising Model: New Developments*, elsewhere in this issue.
54. R. B. Griffiths, Correlations in Ising ferromagnets. I, *J. Math. Phys.* **8**:478–483 (1967).
55. R. B. Griffiths, Correlations in Ising ferromagnets. II. External magnetic fields, *J. Math. Phys.* **8**:484–489 (1967).
56. J. Ginibre, Simple proof and generalization of Griffiths' second inequality, *Phys. Rev. Lett.* **23**:828–830 (1969).
57. M. Widom, Short- and long-range icosahedral order in crystals, glass, and quasicrystals, in *Introduction to Quasicrystals*, Aperiodicity and Order, Vol. 1, M. V. Jarić, ed. (Academic Press, Boston, 1988), pp. 59–110.
58. D. R. Nelson and M. Widom, Symmetry, Landau theory and polytope models of glass, *Nucl. Phys. B* **240[FS12]**:113–139 (1984).
59. J. F. Sadoc and R. Mosseri, Icosahedral order, curved space and quasicrystals, in *Extended Icosahedral Structures*, Aperiodicity and Order, Vol. 3, M. V. Jarić and D. Gratias, eds. (Academic Press, Boston, 1989), pp. 163–188.
60. M. Baake, U. Grimm, and C. Pisani, Partition function zeros for aperiodic systems, *J. Stat. Phys.* **78**:285–297 (1995).
61. P. Repetowicz, U. Grimm, and M. Schreiber, High-temperature expansion for Ising models on quasiperiodic tilings, *J. Phys. A* **32**:4397–4418 (1999).